Polymer Chemistry

ROYAL SOCIETY OF CHEMISTRY

REVIEW

View Article Online
View Journal | View Issue

Cite this: *Polym. Chem.*, 2021, **12**, 1598

Self-healing elastomers based on conjugated diolefins: a review

Prasanta Kumar Behera, Subhra Mohanty and Virendra Kumar Gupta *

Received 13th October 2020,
Accepted 25th February 2021

DOI: 10.1039/d0py01458c

rsc.li/polymers

The formation of microcracks is a common problem in elastomeric materials. The propagation of microcracks to bigger cracks results in the failure of the elastomeric material, which needs to be replaced by a new material, thus creating a huge elastomer waste. The introduction of self-healing property into the elastomeric material is an important way to repair microcracks and to stop the crack propagation process. This review summarizes the progress in self-healing elastomers (polybutadiene rubber, styrene–butadiene rubber, polyisoprene rubber, butyl rubber, nitrile butadiene rubber, chloroprene rubber, and silicon rubber) based on conjugated diolefins. The use of various self-healing mechanisms and their effect on the self-healing property as well as reprocessability has been discussed. The challenges and future research opportunities are highlighted.

1. Introduction

In today's society, rubbers (elastomers) have been used in various fields such as tires, shoes, seals, and many elastomeric products.[1–5] The rise in the demand for rubber products drives the increased production of rubber materials. When the rubber material gets damaged, it needs to be replaced and reprocessed.[6–8] As rubber materials are permanently crosslinked, it is difficult to reprocess and decompose thermally at high temperatures (400–700 °C).[9–11] The growing demand for rubber products and the problem in their reprocessability cause huge rubber wastes.[12] Thus, it is a big challenge for the research community to come up with a solution to this problem.

The solution to the above problem can be achieved in two ways. The first solution is to make the crosslinked rubber reprocessable and the second one is to improve the application life by making them self-healable.[13,14] Making the rubber materials self-healable is a better way to overcome the hurdle as the damaged rubber article does not need to be replaced and remoulded (reprocessed). In recent years, the significant effort by the research community for the development of self-healing rubber gives a new hope to overcome the technological and environmental issues associated with crosslinked rubber wastes.[15] Making rubber self-healable will improve its application life and hence reduce rubber waste. When a crack is

Polymer Synthesis & Catalysis Group, Reliance Research and Development Center, Reliance Industries Limited, Navi Mumbai 400701, India.
E-mail: Virendrakumar.Gupta@ril.com

Prasanta Kumar Behera

Dr Prasanta Kumar Behera received his MTech degree in Rubber Technology and PhD in Polymer Chemistry from Indian Institute of Technology Kharagpur, India. He is currently working as Research Scientist in Research & Development, Reliance Industries Limited. His area of research primarily focuses on the synthesis of functional polymers and their applications in designing self-healing/shape-memory materials and superhydrophobic coatings.

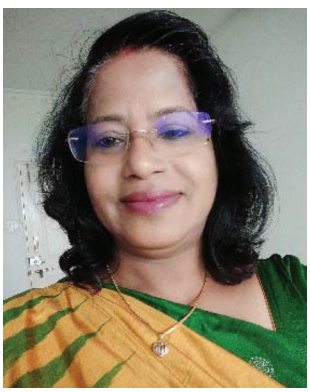

Subhra Mohanty

Dr Subhra Mohanty is currently working as Asst. Vice President in Research and Development of Reliance Industries. She acquired her PhD degree in Rubber Technology from Indian Institute of Technology, Kharagpur, India. She has about 25 peer reviewed publications and 15 patents to her credit. Her research interests are mostly on various functional polymer synthesis and the development of new applications.

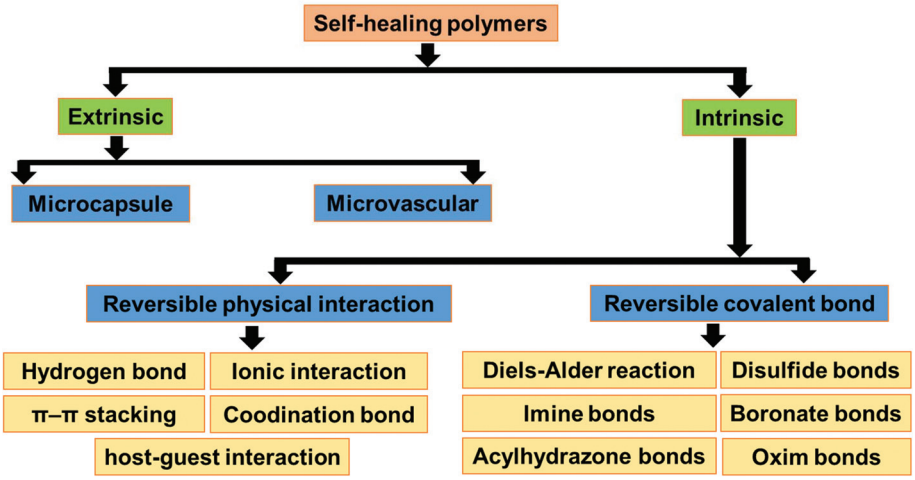

Fig. 1 Classification of self-healing polymers based on the mechanism of the healing process.

generated in the self-healing rubber, it repairs the crack by itself or by application of external stimuli.[16,17] Thus, there is no need to replace the self-healing rubber again and again.

Most rubber-based wastes are generated from tire and automotive applications.[18] Conjugated diolefin based elastomers such as polybutadiene (PB, BR, butadiene rubber), styrene–butadiene rubber (SBR), polyisoprene rubber (IR) (natural rubber, NR), butyl rubber (IIR), nitrile butadiene rubber (NBR), and chloroprene rubber (CR) are widely used in tire, tube, and other automotive applications.[19–22] The lifetime of tire and other rubber articles can be improved by making these rubbers self-healable. Most self-healing polymeric systems are based on dynamic covalent networks or supramolecular interactions.[23,24] The presence of a dynamic network further helps in the reprocessing of rubber materials. Thus, it is important to review the self-healing systems based on PB, SBR, NR, IIR, NBR, and CR, which will help in the design of rubber-based products with interesting self-healing and reprocessable properties. In this review, various self-healing approaches used in the conjugated diolefin based elastomeric system are discussed. The effect of different self-healing mechanisms on the self-healing efficiency and recyclability have been described.

Virendra Kumar Gupta

Dr Virendra Kumar Gupta is currently Head, R&D Polymer, Reliance Industries Limited. He received his Ph.D. in Chemistry from Banaras Hindu University, Varanasi. His current research interests include material science, circular economy, and sustainability. He has 160 patents, 75 research publications and 80 presentations in conferences. He has successfully commercialized 25 technologies in the area of polymers.

2. Various types of self-healing approaches

The self-healing approaches in polymers can be broadly classified into two categories, *i.e.*, extrinsic and intrinsic approaches (Fig. 1).[25] In the extrinsic self-healing approach, the polymer itself does not exhibit self-healing property. Thus, external healing agents are incorporated to induce the self-healing property in the polymer.[26–28] In the intrinsic self-healing system, the polymer does not need any external healing agent. The reversible interaction between the functional groups present in the polymer is the reason behind the self-healing property.[29–31] The functional groups in intrinsic self-healing polymers interact through reversible non-covalent interactions (hydrogen bonding,[32,33] ionic interactions,[34–36] π–π interactions,[37,38] coordination bond,[39] and host–guest interactions[40]) or reversible (dynamic) covalent bond formation (*e.g.*, Diels Alder & retro-DA reaction,[41–49] Alder–ene reaction,[50,51] reversible electrophilic substitution,[52] reversible cyclodimerization,[53–55] disulfide metathesis reaction,[56–58] and boronate ester bearing B–N dative bond[59]). Depending on the nature of the healing agent or the functional moieties present in it, the extrinsic and intrinsic approaches may be autonomous or non-autonomous (Fig. 2).[60–62] Autonomous self-healing means it does not need an external stimuli, while the non-autonomous self-healing system needs external stimuli to show the self-healing property.

3. Self-healing polybutadiene (PB)

The presence of the main chain and pendant double bonds in PB makes it a suitable rubber for further modification. Different functional groups are incorporated into the PB

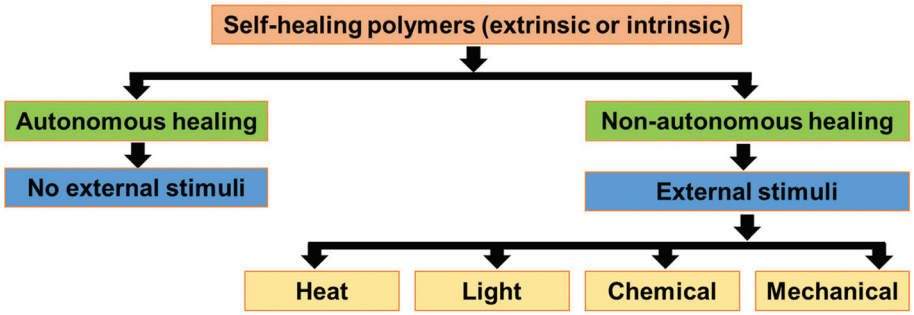

Fig. 2 Classification of self-healing polymers based on the stimuli required for the healing process.

rubber *via* reaction with the pendant as well as the main chain double bond.[63–66] The grafting of suitable functional groups onto PB may help in showing its self-healing property.

3.1. Self-healing PB *via* Diels–Alder (DA) and retro Diels–Alder (DA) reactions

DA and rDA reactions are the most versatile mechanisms to develop self-healing polymers (Fig. 3). A diene and a dienophile are needed to prepare the self-healing PB *via* DA and rDA approach. Dienes or dienophiles are grafted onto the PB chain and then the crosslinking reaction is performed *via* the DA reaction. The covalent crosslinks formed *via* the DA reaction break at high temperature (110–160 °C) and the formation of DA adducts takes place when the temperature is reduced to 55–75 °C. When cracks appear, the rubber is heated above the rDA reaction temperature, which leads to the breaking of DA adducts. The further reduction of the temperature to 55–75 °C results in the formation of DA adducts and heals the cracks.

Polybutadienes can be easily functionalized *via* the thiol–ene reaction using furfuryl thiol. In comparison to the *cis*/*trans* units, the vinyl groups are more reactive toward the thiol–ene reaction.[67] Trovatti *et al.*[68] reported the preparation of a crosslinked PB rubber using the DA reaction and claimed that this strategy can be utilized to develop a recyclable tire. First, the furan-functionalized PB is prepared *via* the thiol–ene reaction and then crosslinked *via* the DA reaction using bismaleimide as a dienophile. On heating above 110 °C, the crosslinked PB undergoes decrosslinking *via* the rDA reaction. Bai *et al.*[69] studied the recyclability and self-healing property of PB rubber prepared by the DA reaction between furan-functionalized PB and bismaleimide (Fig. 4). The crosslinked elastomer exhibits good recyclability and can be thermally remoulded to produce a new sample without a significant impact on the mechanical properties. The crack in the crosslinked rubber starts to decrease at 90 °C and completely disappears when the temperature reaches above 150 °C. This indicates that the crosslinked PB rubber shows self-healing behavior at high temperature.

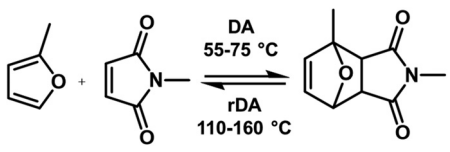

Fig. 3 Schematic representation of Diels–Alder (DA) and retro Diels–Alder (rDA) reaction in furan and maleimide systems.

Besides the thiol–ene reaction, other alternative methods have also been reported to incorporate DA moieties into PB rubber. Berto *et al.*[70] reported a three-step method to prepare a tetrafuran telechelic *cis*-1,4-PB rubber (Fig. 5). They first prepared the epoxidized PB rubber *via* the epoxidation of PB using *m*-CPBA (*meta*-chloroperoxybenzoic acid), which on treatment with periodic acid gave the aldehyde telechelic PB rubber with different chain lengths (low molecular weight). The aldehyde telechelic PB is then functionalized with diethanolamine (DEA) to prepare tetrahydroxyl telechelic PB, which on further reaction with furfuryl isocyanate, give a tetrafuran-functionalized telechelic PB. The reaction of the liquid-like furan-functionalized PB with bismaleimide *via* DA chemistry results in the formation of elastomeric networks. The tensile strength of the DA crosslinked product is highly dependent on the molecular weight of the furan telechelic PB. Low molecular weight oligomers exhibit higher tensile strength and lower elongation at break, which is due to the increased crosslink density. Interestingly, these materials can be recycled over five times without a loss in their mechanical properties.

3.2. Self-healing PB *via* disulfide metathesis reaction

Similar to DA and rDA click reactions, the disulfide metathesis reaction is also based on a dynamic covalent bond, as shown in Fig. 6. The disulfide moieties present in rubber can undergo disulfide metathesis reaction at room temperature or under external stimuli (temperature or UV light). The exchange of polymer segments *via* the disulfide metathesis reaction results in the self-healing property.

Xiang *et al.*[71] reported the preparation of a self-healable and reprocessable PB rubber by thiol–ene photo-click polymerization between the double bonds in PB and thiols in polysulfide (Fig. 7). Under UV irradiation, the rearrangement of the crosslinked network takes place *via* the disulfide metathesis reaction, which induces the self-healing property in the rubber. The healing efficiency increases with an increase in the content of disulfide bonds. The increase in the intensity of

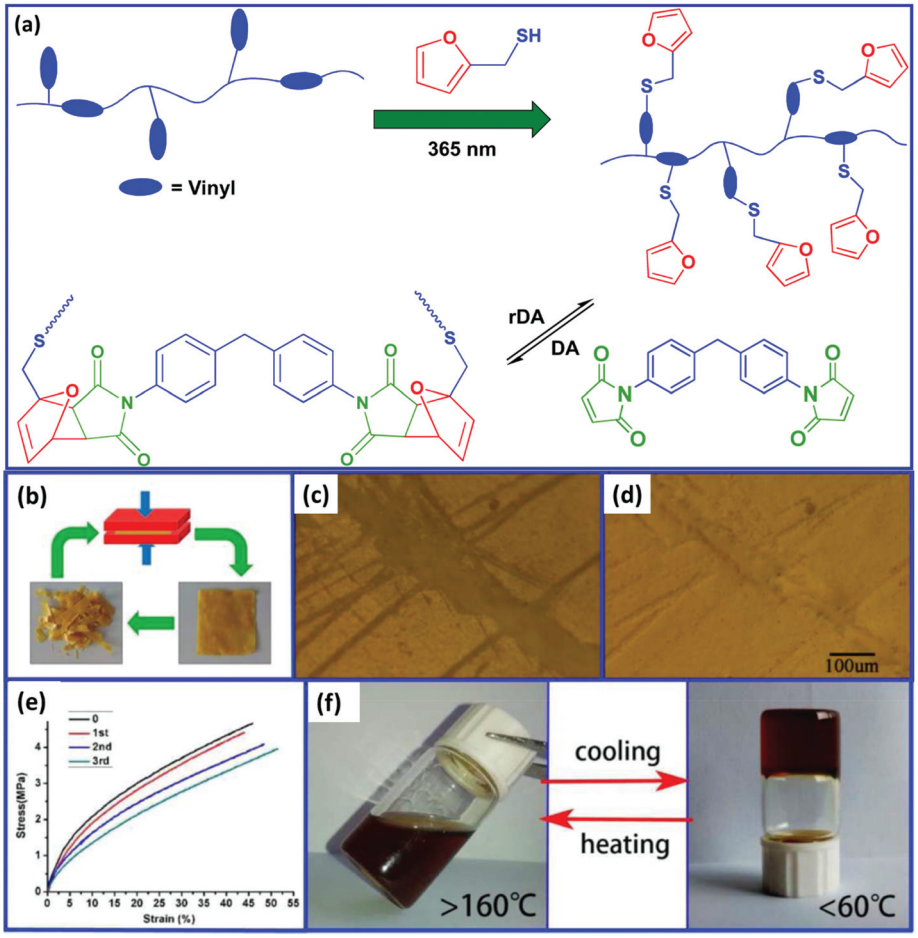

Fig. 4 (a) Schematic representation for the preparation of the recyclable PB rubber, (b) recyclability study, (c) the photograph of the scratched film at room temperature, (d) the photograph of the film after healing at 150 °C, (e) stress–strain curves of the pristine and the recycled samples, and (f) the sol–gel process in dichlorobenzene at different temperatures.[69] Reproduced from ref. 69 with permission from American Chemical Society, copyright 2015.

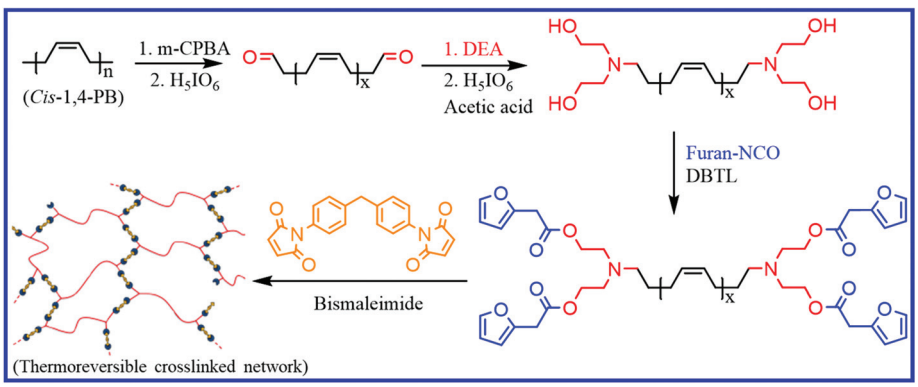

Fig. 5 Schematic representation of the preparation of furan telechelic PB rubber and its DA adduct.[70] Reproduced from ref. 70 with permission from American Chemical Society, copyright 2018.

the UV light and the time of irradiation also improves the healing efficiency. The conventional sulfur-crosslinked PB rubber can also be made self-healable and recyclable by triggering the disulfide rearrangement reaction with a suitable catalyst. Xiang *et al.*[72] reported the use of $CuCl_2$ to catalyze the disulfide metathesis reaction in sulfur-crosslinked PB rubber.

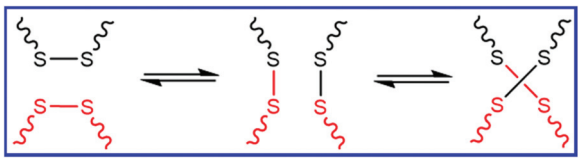

Fig. 6 Schematic representation of the disulfide metathesis reaction.

The catalyst is incorporated in the rubber during compounding, which accelerates the disulfide exchange reaction. The sulfur-crosslinked PB with 0.1 phr of $CuCl_2$ shows a healing efficiency of 75% when healed at 110 °C for 12 h, whereas the sulfur-crosslinked PB without $CuCl_2$ exhibits a healing efficiency of only 12%. This indicates that $CuCl_2$ catalyzes disulfide metathesis through a circulated crossover reaction between the disulfide and polysulfide bonds. Interestingly, the incorporation of $CuCl_2$ also helps in the reprocessing of sulfur-crosslinked rubber.

3.3. Self-healing PB *via* hydrogen bonding, ionic interaction, and crystallization

Self-healing PB rubber can be prepared by the introduction of functional groups that undergo reversible ionic association, hydrogen bonding, or crystallization. Wang *et al.*[73] studied the effect of the combination of covalent and non-covalent crosslinks on the self-healing, shape-memory, and mechanical properties of PB rubber. They prepared the self-healing PB elastomer *via* the self-assembly of PB oligomers having carboxylic acid and amine groups, followed by covalent crosslinking *via* the thiol–ene reaction (using a tri-functional thiol compound) (Fig. 8). The interaction between the carboxylic acid and the amine groups results in the formation of dynamic ionic-hydrogen bonds and induced the self-healing property in the elastomer. At low covalent crosslinking density, these PB show self-healing properties at room temperature. The increase in the covalent crosslink density improves the shape-memory and mechanical properties but reduces the self-healing efficiency.

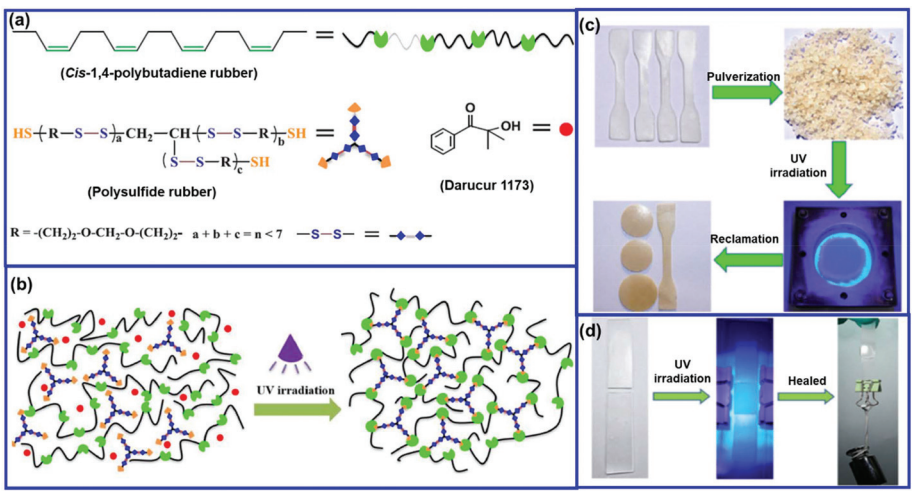

Fig. 7 (a) Chemical structures of the main components of UV-curable PB rubber, (b) photocrosslinking process in the UV-curable rubber, (c) reprocessing of the cured rubber, and (d) photographs illustrating the healing processes of the UV-cured rubbers.[71] Reproduced from ref. 71 with permission from Elsevier, copyright 2019.

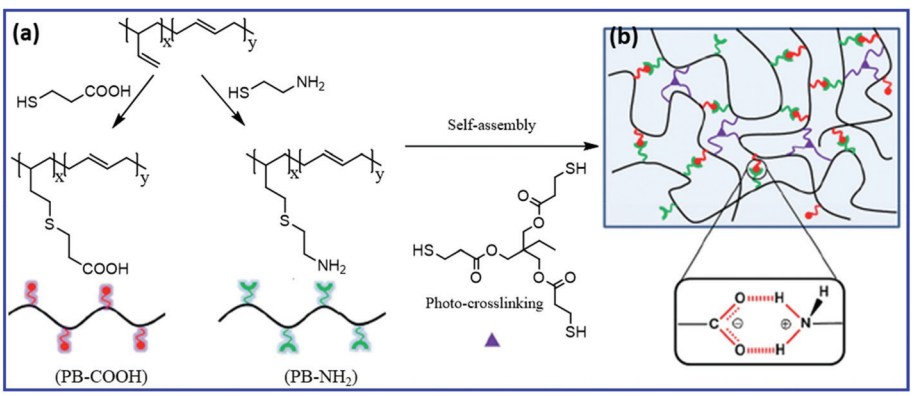

Fig. 8 (a) Schematic representation of the preparation of –COOH and $-NH_2$ functionalized PB *via* the thiol–ene reaction. (b) The polymer network having both ionic hydrogen bonds and covalent cross-links.[73] Reproduced from ref. 73 with permission from Royal Society of Chemistry, copyright 2015.

Without a crosslinker, the healing efficiency is about 93% and decreased to 77% and 33% with the increase in the crosslinker concentration to 2% and 6%, respectively. The presence of irreversible covalent crosslinks reduces the chain mobility, which in turn reduces the healing rate and healing efficiency.

Jasra *et al.*[74] introduced the concept of hydrogen bonding in the preparation of a thermoreversible and self-healing PB rubber blend. They prepared the self-healing PB *via* blending PB rubber with maleic anhydride-grafted polypropylene, followed by the ring-opening of the maleic anhydride group using triazole derivatives such as 3-amino-1,2,4-triazole and 4-amino-1,2,4-triazole. The carbonyl groups involved in the formation of thermo-reversible hydrogen bonding with amine and carboxylic acid protons which help the blend to show self-healing properties in the temperature range of 40–85 °C.

The grafting of crystallizable hydrocarbons onto PB can impart self-healing property. The crystallizable hydrocarbon side chains in PB will undergo association to form crystalline domains. These crystalline domains will melt on heating and again recrystallize on reducing the temperature. The melting and reformation of crystallites will act as a reversible network and induce self-healing property in the elastomer. Xu *et al.*[75] reported the preparation of thermoresponsive self-healing PB coatings by the grafting of 1*H*,1*H*,2*H*,2*H*-perfluorodecanethiol (PFDT) onto vinyl pendant groups of 1,2-PB *via* thiol–ene reaction. PB-g-PFDT exhibits a glass transition at 44 °C and a melting transition at 68 °C. When the scratched coating surface of PB-g-PFDT is healed at 50 °C for 50 min, no significant change in the scratch is observed. Although the chain mobility of PB-g-PFDT is improved above the T_g, the crystallites of PFDT still restrict the migration of the polymer chains to the scratched area. Interestingly, the scratch on this coating completely disappeared when healing was performed at 80 °C for 5 min, followed by cooling down to room temperature. At 80 °C, the melting of the PFDT crystallites occurs and further reduction in temperature results in the reformation of the crystallites, which leads to the complete healing of the scratch. This PB-g-PFDT coating also exhibits anti-smudge property and various liquids (with a wide range of surface tensions) readily slide off the coating surfaces without leaving any residue. In addition to other flat surfaces, PB-g-PFDT can also be used on cotton fabrics to prepare superamphiphobic fabrics that are capable of repetitively healing the damage.

Self-healing properties are of utmost importance in PB rubber as these are mostly used in the sidewall of a tire. In the event of any cut/puncture in the sidewall, the tire is discarded. The inbuilt self-healing properties of PBR is one of the most desired properties in the automotive segment. In this section, self-healing PB has been discussed using various mechanisms such as the DA/rDA reaction, disulfide metathesis reaction, hydrogen bonding, ionic interaction, and side-chain crystallization. Semicrystalline polycaprolactone oligomers can also be grafted onto PB rubber and their impact on the self-healing property could be evaluated. From the multiple literature studies of various methodologies, it is concluded that the functionalization of PB rubber is more suitable from the process prospective, which imparts self-healing characteristics under specific conditions.

4. Self-healing styrene–butadiene rubber (SBR)

SBR is a synthetic rubber comprising styrene (10–25%) and butadiene (75–90%) monomers. The butadiene unit in SBR is approximately composed of 60 to 70% *trans*-1,4; 15 to 20% *cis*-1,4; and 15 to 20% 1,2 configurations at 50 °C. High styrene and high vinyl grades are also available for special applications.[76] Carboxylated SBR (XSBR) is a modified grade of SBR, which contained pendant –COOH groups.[77] The –COOH groups in XSBR can be easily utilized to design self-healing rubber.[78]

The introduction of non-covalent supramolecular networks is an important way to design self-healable and recyclable rubber materials. In most cases, the non-covalent supramolecular networks do not impart good mechanical properties and make them inferior for certain applications. To overcome this difficulty, Xu *et al.*[79] prepared a self-healing carboxylated SBR *via* the reaction between carboxyl groups of carboxylated SBR (XSBR) and zinc oxide (ZnO), where Zn^{2+} acts as a crosslinker between the XSBR molecules (Fig. 9). Secondary ionic networks are also formed *via* further self-aggregation of the ion pairs of Zn^{2+} salts, whose rearrangements results in good recycling ability. Interestingly, pristine XSBR with 5 wt% zinc oxide exhibits a tensile strength of 6.7 MPa (increased to 10.3 MPa after 3 recycles), which is far higher than that of the most reported non-covalent supramolecular rubbers.

The functional groups on nanoparticles also interact with the –COOH group of XSBR and result in the self-healing property. Xu *et al.*[80] prepared self-healing carboxylated styrene–butadiene rubber (XSBR)/nano-chitosan (NCS) composites *via* the salt-forming reaction, in which NCS is responsible for constructing the supramolecular hybrid network (Fig. 10). The $-NH_2$ group of NCS interacts with the –COOH group of XSBR, which results in the formation of carboxylate ammonium salt ($[COO^-][NH_3^+]$). The carboxylate ammonium groups further aggregate to form week ionic clusters, which are responsible for the self-healing property. In XSBR/NCS composites, NCS acts as a multifunctional crosslinker and improves the mechanical properties without sacrificing the self-healing property. With 20 wt% NCS loading, the tensile strength of the XSBR/NCS composite increases twice that of pristine XSBR and the healing efficiency is found to be 92% after healing at room temperature for 24 h. The NCS loading strongly affects the healing efficiency of the XSBR/NCS composites. The self-healing efficiency continuously increases up to 20 wt% of NCS loading, which is due to the increase in the ionic bond crosslinks in the supramolecular hybrid network. A further increase in the NCS loading (30% and 40%) significantly reduces the healing efficiency. The decrease in the healing efficiency at higher filler loading is due to the formation of the filler-filler network, which hinders the mobility and the interfacial interpenetration of the XSBR molecular chains, and reconstitution of ionic bond crosslinks.

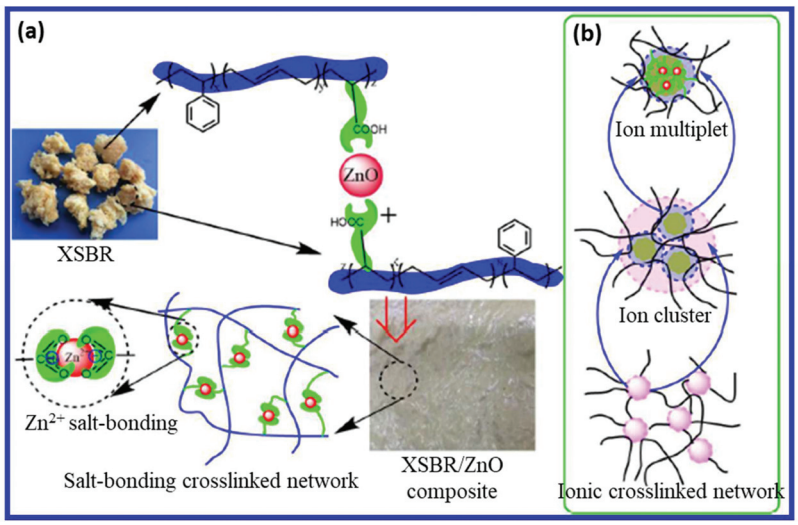

Fig. 9 (a) Schematic representation of network formation by the reaction between carboxyl groups of XNBR and zinc oxide. (b) Schematic for ion multiplet, ion cluster, and ionic crosslinked network.[79] Reproduced from ref. 79 with permission from American Chemical Society, copyright 2016.

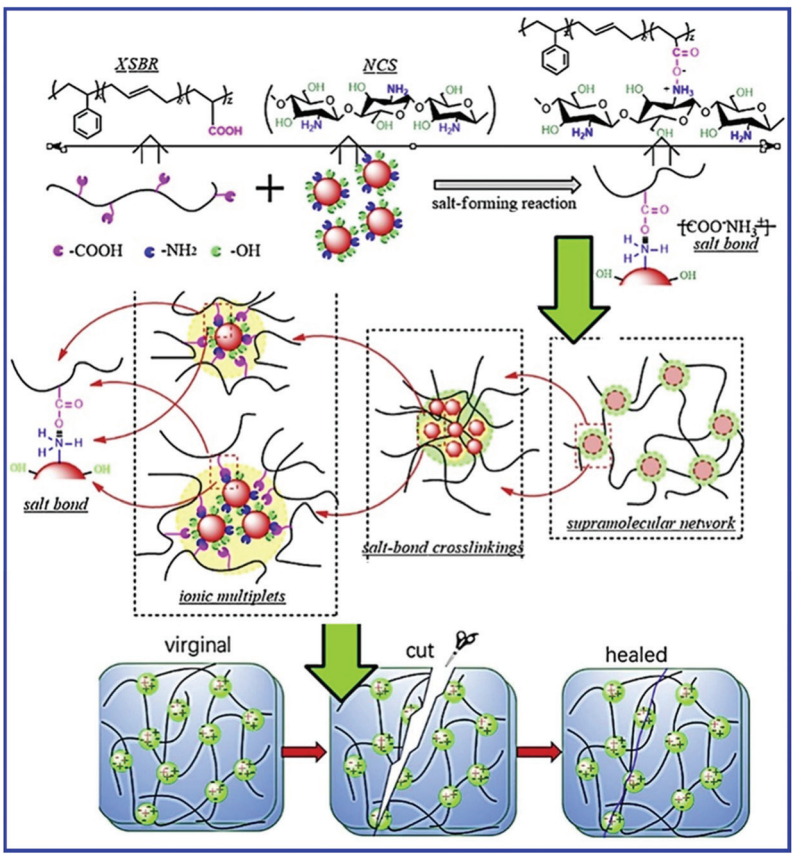

Fig. 10 Schematic representation of salt-forming reaction between XSBR and NCS, the evolution of the supramolecular hybrid network in the XSBR/NCS composites, and self-healing by the reestablishment of ionic bond crosslinking in the supramolecular XSBR network.[80] Reproduced from ref. 80 with permission from Elsevier, copyright 2019.

Besides chitosan, multiwall carbon nanotube (MWCNT) also have a great impact on the self-healing and mechanical properties of SBR. Kuang *et al.*[81] reported the preparation of self-healing SBR/CNT nanocomposites *via* the DA and rDA approaches. In this case, the furfuryl-grafted SBR (SBR-FS) and furfuryl-terminated MWCNT (MWCNT-FA) react with bismalei-

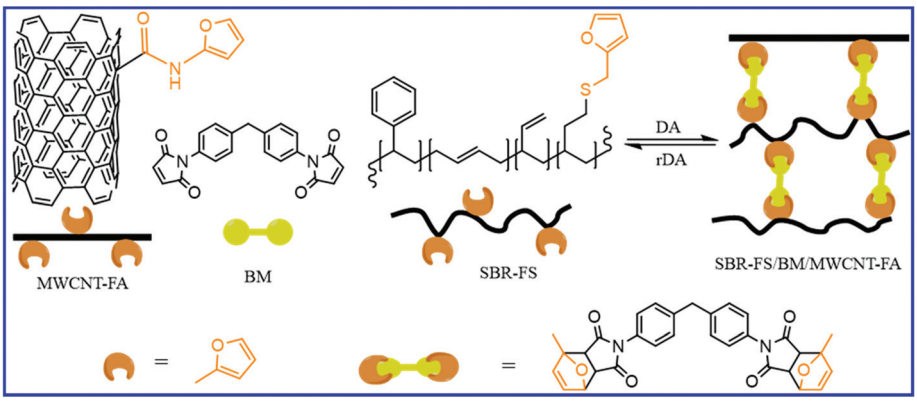

Fig. 11 Schematic representation for the preparation self-healable SBR-FS/BM/MWCNT-FA nanocomposites *via* DA reaction of the furan group of rubber and CNT with bismaleimide.[81]

mide (BM) to form covalently bonded and reversibly cross-linked rubber composites (Fig. 11). The Young's modulus of the SBR-FS/BM/MWCNT-FA increases by 200–300% with just 5 wt% loading of MWCNT-FA. The tremendous increase in the modulus is because of the increase in the crosslink density as well as the reinforcing effect of the MWCNT-FA. The increase in MWCNT-FA further improves the healing efficiency. Thus, MWCNT-FA plays a dual role in improving the healing efficiency and mechanical properties *via* the formation of DA adducts with BM as well by acting as the reinforcing filler. The effect of the MWCNT-FA content on the healing efficiency is highly dependent on the furan/maleimide ratio. The incorporation of 5 wt% MWCNT-FA in SBR-FS/BM (with furan/maleimide ratio of 3 : 1) improves the healing efficiency from 37% to 90% when heated at 100 °C for 5 h. In SBR-FS/BM, where the furan/maleimide ratio is 1 : 1, the healing efficiency decreases with the addition of 5 wt% MWCNT-FA. The decrease in the healing efficiency is due to the increased crosslink density, which reduces the mobility of the polymer chains. The healing efficiency of the MWCNT-FA based composite is much higher than that of the MWCNT-COOH (–COOH functionalized MWCNT) because the –COOH functional groups in MWCNT-COOH do not take part in the DA and rDA reaction. The crosslinked SBR-FS/MWCNT-FA/BM nanocomposites are reprocessable similar to thermoplastic elastomers on heating to about 130–150 °C.

A few works have been reported in the area of self-healing SBR, which is having the single largest synthetic rubber application in the rubber industry. High styrene content SBR or hydrogenated SBR with self-healing property will further widen the application areas of SBR.

5. Self-healing polyisoprene rubber (IR) (Natural rubber-NR and synthetic IR)

Natural polyisoprene rubber (NR) and synthetic polyisoprene rubber (IR) are composed of *cis*-1,4-polyisoprene.[82] The *cis*-1,4 isoprene content in NR is higher than that of IR.[83,84]

5.1. Self-healing IR *via* the DA and rDA reaction

Natural polyisoprene rubber (NR) is one of nature's most exceptional materials, which is predominantly used in the tire industry. NR can be made self-healable by grafting a suitable functional moiety on its backbone. Tanasi *et al.*[85] prepared a furan-functionalized NR (NR-g-furan) by grafting furfuryl amine molecules onto the maleic anhydride-functionalized NR (NR-g-MA) (Fig. 12). The DA reaction between the furan groups of furan-functionalized NR and the maleimide groups of bismaleimide gives a crosslinked NR (NR-DA). The crosslinked NR is thermoreversible and shows self-healing property when heated to the rDA and DA temperature. These samples show a healing efficiency of 38–85% after healing at 130 °C for 4 h, followed by another 3–7 h at 40 °C.

5.2. Self-healing IR *via* ionic network

Introducing ionic interactions is one of the important ways to design self-healing isoprene rubbers. Miwa *et al.*[86] reported the preparation of self-healing IR by introducing carboxyl groups to 1.7% of the repeating units, followed by neutralization of 24–90% of the carboxyl groups with sodium hydroxide (Fig. 13a). The association of the ionic group forms a network structure where the ionic moieties undergo continuous hopping between the ionic aggregates at room temperature. This ionic hopping makes the network dynamic and results in self-healing property at room temperature (28 °C). The rate of ionic-hoping of the ionomers increases with decreasing neutralization level, which in turn improves the healing rate. Carboxylated *cis*-IR with 55% neutralization shows ~80% recovery after 6 h at room temperature, whereas more than 40 h is required for carboxylated IR with 90% neutralization. At the same neutralization levels, the self-healing rate decreases with the increase in the molecular weight, which is due to the reduction in the diffusion and randomization of the polymer chains between the damaged faces.[87] Interestingly, the introduction of ionic moieties to *trans*-IR (*via* 90% neutralization of carboxyl groups) does not result in the self-healing property at room temperature. The blending of ionically-modi-

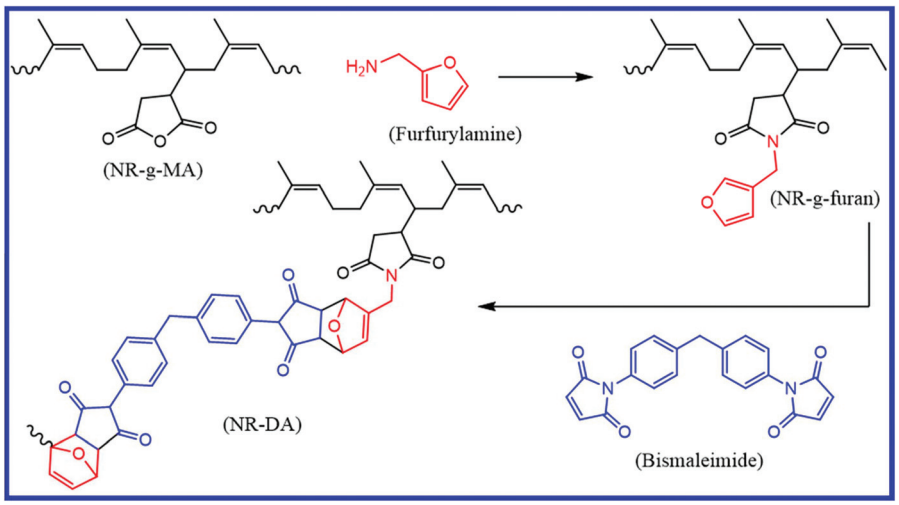

Fig. 12 Schematic representation of the preparation of furan-functionalized NR and the crosslinking of furan-functionalized NR *via* the DA reaction using bismaleimide.[85] Reproduced from ref. 85 with permission from Elsevier, copyright 2019.

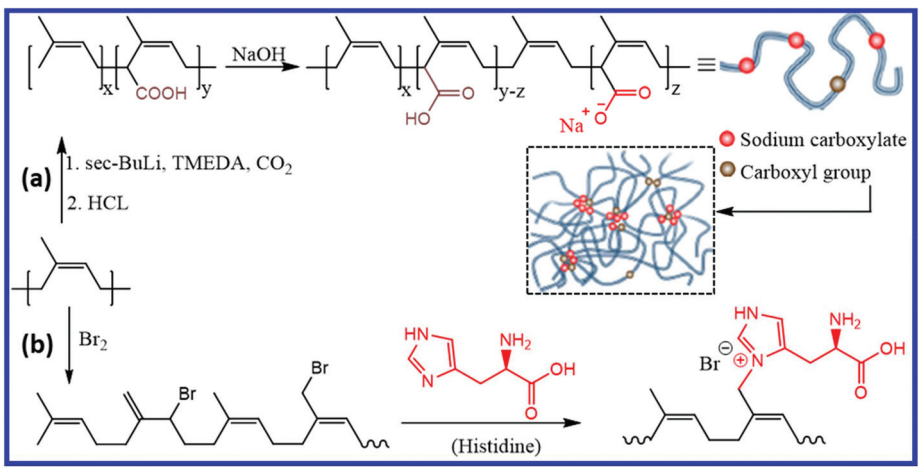

Fig. 13 (a) Schematic illustration of the preparation of sodium carboxylate-functionalized IR and ionic association in it.[86] (b) Schematic representation of the preparation of self-healing NR ionomer from brominated NR.[89] Reproduced from ref. 86 with permission from Springer Nature, copyright 2019. Reproduced from ref. 89 with permission from Elsevier, copyright 2020.

fied *trans*-IR with ionically-modified *cis*-IR improves the modulus with a reduction in the self-healing efficiency.[88] Yang *et al.*[89] reported a facile method for the preparation of the self-healing NR ionomer by reacting brominated NR with histidine (Fig. 13b). The strong ionic interaction between the ionic moieties results in a physically crosslinked elastomer with faster healing time (~10 s) and a significant self-healing efficiency (93.98%).

The strength of the rubbers based on an ionic cross-linking network is quite limited and their long-term dimensional stability is questionable. Thus, it is important to incorporate both ionic and covalent crosslinks to develop self-healing rubber with good mechanical properties. Xu *et al.*[90] reported the preparation of a potential self-healing material *via* controlled peroxide-induced vulcanization to generate massive ionic crosslinks *via* the polymerization of zinc dimethacrylate (ZDMA) in NR. They controlled the vulcanization process to generate reversible supramolecular networks *via* ionic crosslinks by retarding the formation of covalent crosslinks. The ionic crosslinks can be easily rearranged between themselves and result in the self-healing property. A fully cut and mended sample nearly gains its original strength when healed at the ambient temperature. In comparison to ZDMA, the use of excess zinc oxide (ZnO) and methacrylic acid (MAA) in NR, where the *in situ* formation of ZDMA takes place during the peroxide curing process, results in better mechanical properties.[91] The improved mechanical properties are due to the presence of residual nano ZnO, which acts as a reinforcing filler and helps in the formation of the new ionic supramolecular hybrid network in the NR/MAA/ZnO compounds.

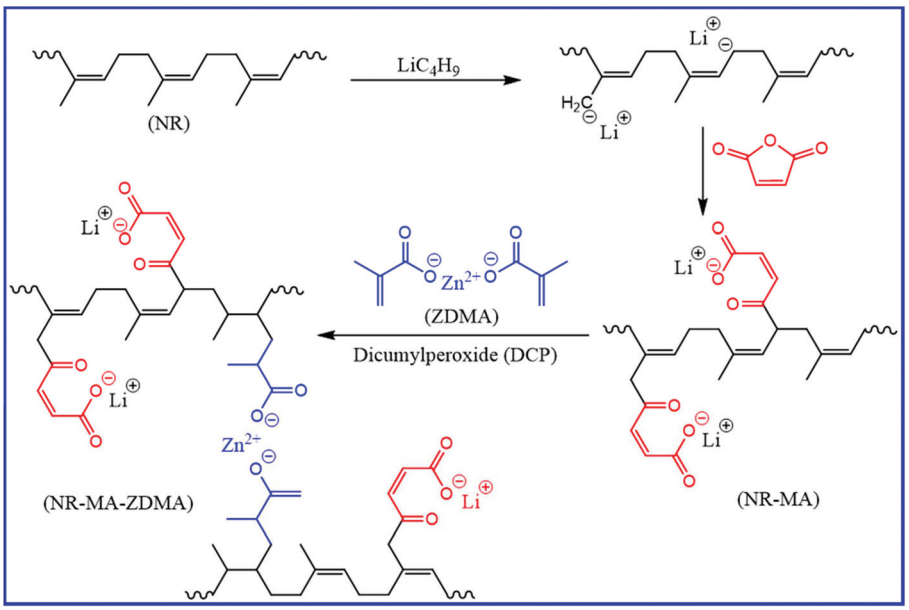

Fig. 14 Schematic representation of the preparation of self-healing NR having a dual ionic network.[92] Reproduced from ref. 92 with permission from American Chemical Society, copyright 2020.

Interestingly, the self-healing efficiency of the NR/MAA/ZnO compounds decreases with an increase in the healing temperature from 23 °C to 80 °C. Although a higher temperature accelerates the mobility of the NR chains across the damaged surface, the seriously deteriorated ionic associations are unable to construct powerful new ionic crosslinks during healing. The ratio of ZnO/MAA in the NR/MAA/ZnO compound also has a strong impact on the mechanical properties and the rate of healing. An increase in the ZnO/MAA ratio improves the mechanical properties and healing efficiency but reduces the rate of healing. To improve the self-healing and mechanical properties, Liu *et al.*[92] incorporated a dual ionic network into NR (Fig. 14). The reaction of lithiated NR with maleic anhydride (MA) generates lithium carboxylate (–COOLi)-based ionic network (NR-MA), which on further reaction with zinc methacrylate (ZDMA) and peroxide results in a second ionic network (NR-MA-ZDMA). As compared to the ZDMA-crosslinked NR, the combination of lithium carboxylate-based network and ZDMA network provides better mechanical and self-healing properties.

Rahman *et al.*[93] reported that at high temperatures, epoxidized natural rubber (ENR) shows the self-repairing property due to the interdiffusion of rubber chains and the strong interaction between epoxy groups. Thus, the incorporation of ZDMA into ENR, followed by crosslinking with peroxide, can further improve the self-healing and mechanical properties of ENR. Liu *et al.*[94] reported the preparation of self-healing rubber *via* controlled peroxide vulcanization of ZDMA (30 phr) filled ENR (ENR/ZDMA). Controlled peroxide vulcanization is performed at a somewhat lower temperature (140 °C) than conventional curing (150 °C), which suppresses the covalent crosslinking of ENR and facilitates the self-polymerization and grafting of ZDMA molecules on to ENR. The self-polymerized and grafted ZDMA form a reversible ionic cluster and induce the self-healing property. The percentage of epoxidation in ENR also affects the self-healing property of the ENR/ZDMA compounds. ENR25/ZDMA (ENR with 25% epoxidation) shows self-healing properties at a lower temperature than that of ENR40/ZDMA (40% epoxidation). After healing at 80 °C for 1 h, the tensile strength of the ENR40/ZDMA composites is recovered to more than 80% of the standard sample, whereas the tensile strength of the ENR25/ZDMA samples is restored to about 70% after healing at room temperature for 50 min. The self-healing property of ENR can also be tuned by blending with a suitable ionomer. Rahman *et al.*[95] studied the self-healing property of the ENR/ionomer blend, where the ionomer is a partially neutralized product of poly(ethylene-co-methacrylic acid) (EM, 15% acid content) with sodium (EMNa) or zinc (EMZn). The ENR/EMNa blend shows complete self-healing, whereas partial self-repairing is observed for the ENR/EMZn blend.

5.3. Self-healing IR based on reversible coordination bond and hydrogen bonding

Self-healing natural rubber can be prepared *via* the introduction of reversible coordinate bonds. ENR and modified ENR with a suitable functional group can form a reversible coordinate bond with different metal atoms. Han *et al.*[96] developed a facile and effective approach to fabricate self-healing NR *via* metal–ligand coordinate bond formation. They modified the commercially available ENR by polydopamine (PDA) and then cross-linked it *via* reversible catechol-Fe^{3+} coordination bonds (Fig. 15a). The resulting Fe^{3+}/PDA-ENR elastomer exhibits good tensile strength (2 MPa) with a self-healing efficiency of 89.3 ±

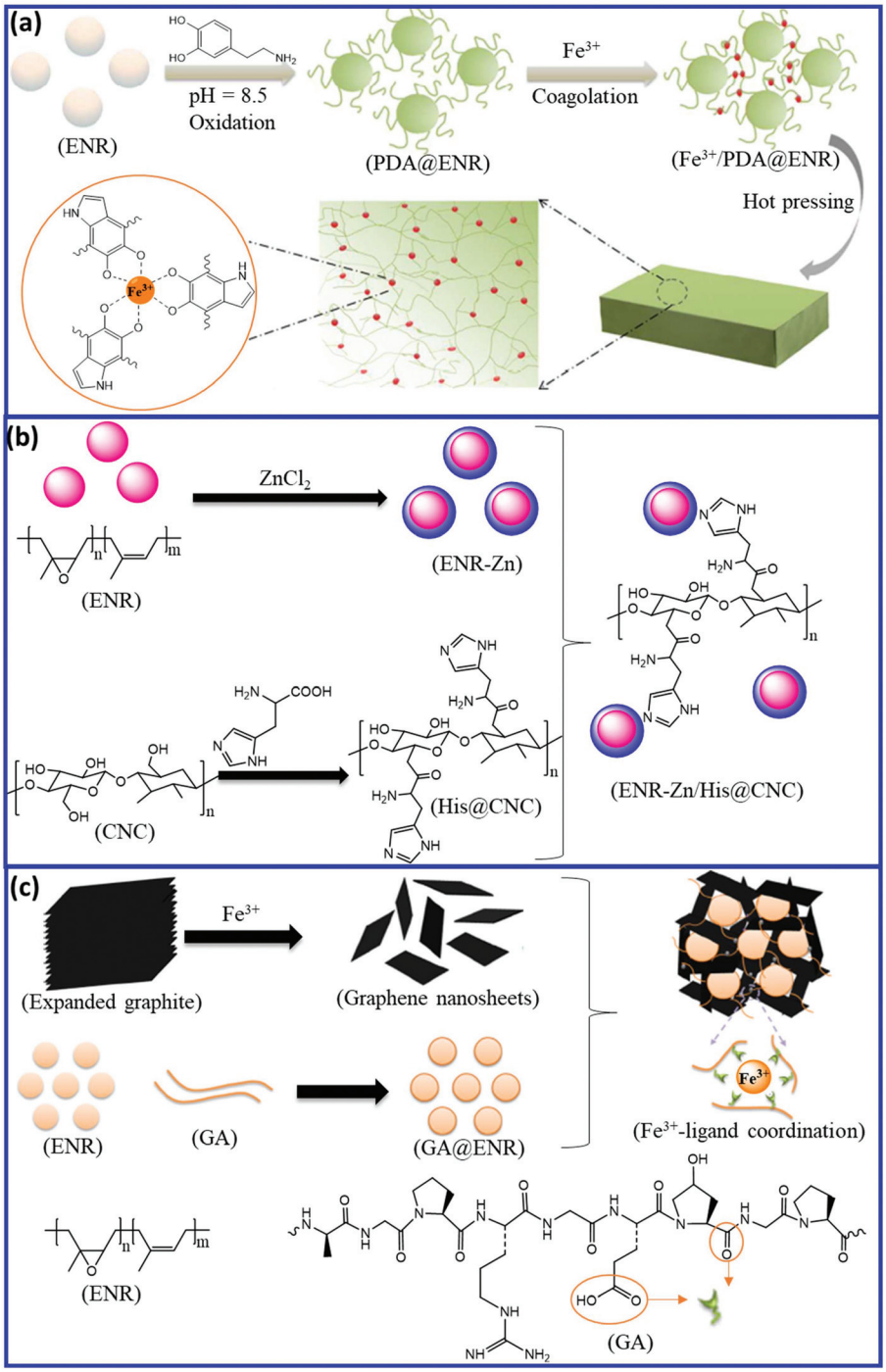

Fig. 15 Schematic representation of the preparation of self-healing ENR *via* reversible coordinate bonds; (a) catechol-Fe^{3+}, (b) histidine-Zn^{2+}, and (c) gelatine-Fe^{3+}.[96–98] Reproduced from ref. 96 with permission from American Chemical Society, copyright 2017. Reproduced from ref. 98 with permission from American Chemical Society, copyright 2019.

3.6% after healing at 50 °C for 12 h. Interestingly, even at low temperature (−10 °C), the Fe^{3+}/PDA@ENR elastomer shows a healing efficiency of ~80% after 12 h of healing. Liu *et al.*[97] reported the preparation of a self-healing blend based on $ZnCl_2$-decorated ENR (ENR-Zn) and histidine (His)-modified cellulose nanocrystal (His-CNC) (Fig. 15b). Histidine and Zn^{2+} form supramolecular metal–ligand coordination, which results in excellent self-healing property with an efficiency of 107.17%, 95.43%, and 88.65% for the first, second, and third cycle, respectively. The ENR-Zn/His-CNC blend exhibits a tensile strength of 1 MPa, which is far lower than that of the Fe^{3+}/PDA-ENR. Tang *et al.*[98] incorporated Fe^{3+}-intercalated gra-

phene nanosheet (Fe^{3+}-GN) into the gelatin-ENR (GA-ENR)-based emulsion to obtain a self-healing elastomer *via* reversible coordination between Fe^{3+} and gelatin (GA) (Fig. 15c). The Fe^{3+}-GN/GA-ENR composite exhibit low tensile strength (1.6 MPa) with a healing efficiency of 94%. It is always challenging to achieve higher self-healing efficiency along with good mechanical properties *via* a reversible coordination mechanism.

The mechanical and self-healing properties of IR and ENR can be improved by introducing a dual dynamic network.[99] Liu *et al.*[100] reported a self-healing polyisoprene *via* the dual-dynamic network by introducing weaker multiple hydrogen bonds and stronger Zn–triazole coordinate bond into the unvulcanized *cis*-1,4-polyisoprene matrix (Fig. 16a). The dual dynamic system results in excellent recovery in the mechanical properties of about 74% (tensile strength before and after healing are 21 MPa and 15.5 MPa, respectively) when it is healed at 80 °C for 24 h. Chen *et al.*[101] introduced coordination as well as boronic ester bonds into ENR to develop a dual dynamic self-healing elastomer. They prepared the dynamic dual crosslinked elastomer by crosslinking ENR using a dithiol-bearing boronic ester crosslinker, followed by the coordination of the epoxy group with Zn^{2+} (Fig. 16b). The network rearrangement through boronic ester transesterifications and reversible Zn^{2+}–O coordination provide excellent healing efficiency (60–100%) and good mechanical properties (1.60 to 14.63 MPa).

5.4. Self-healing IR and epoxy-functionalized IR based on dynamic disulfide metathesis

Polydiene rubbers including NR (IR) are mostly cured using the sulfur vulcanization process. The sulfur vulcanization process creates sulfur crosslinks of different lengths (mono-, di-, and poly-sulfide bonds), pendant side groups, and cyclic sulfides. Depending on the accelerator/sulfur (a/s) ratio, the sulfur vulcanizations are generally classified as conventional (CV, a/s = 0.1–0.6), semi-efficient (semi-EV, a/s = 0.7–2.5), and efficient (EV, a/s = 2.5–12).[102–104] The CV system, where the a/s ratio is low, forms more disulfide and polysulfide linkages, whereas the EV system results in more monosulfide linkages. The disulfide and polysulfide bonds can undergo disulfide exchange reactions and induce the self-healing property in the elastomer. Hernández *et al.*[105] prepared self-healing NR using the conventional sulfur curing system with a low a/s ratio (0.2). At a constant a/s ratio (0.2), the increase in the sulfur content (from 0.7 phr to 2.5 phr) reduces the healing efficiency, which is due to the increased crosslink density of the system. The increased crosslink density reduces the chain mobility, which

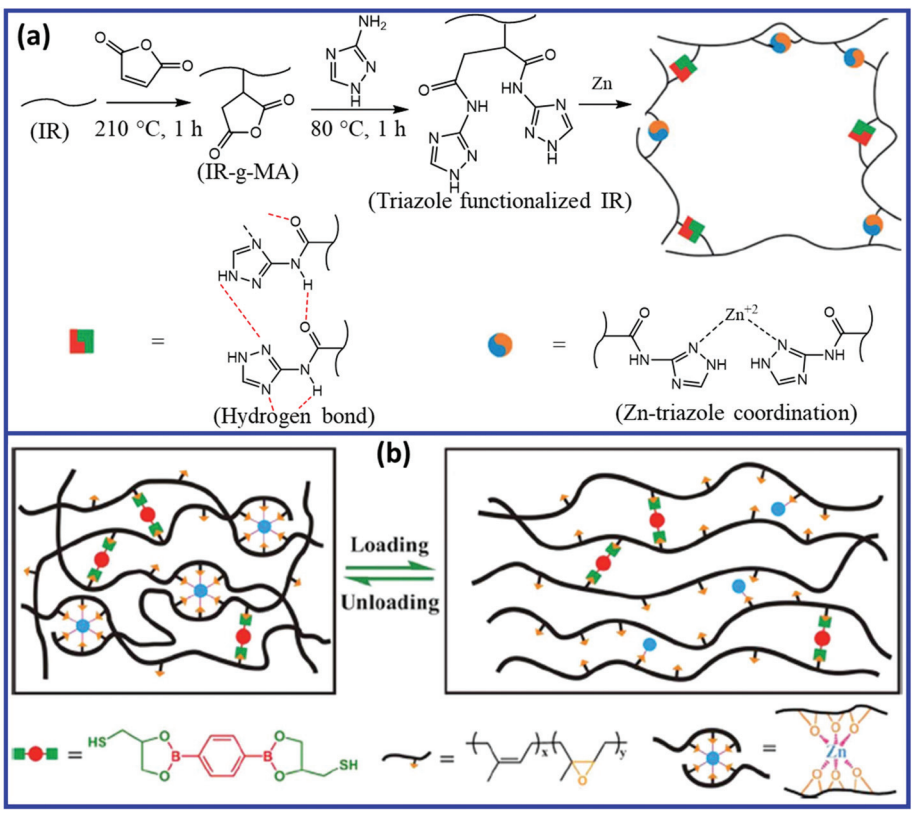

Fig. 16 (a) Schematic representation of the preparation of self-healing IR *via* a dual dynamic network based on reversible hydrogen and coordinate bond.[100] (b) Self-healing ENR networks with dual dynamic crosslinks of boronic ester bonds and non-covalent Zn^{2+}–O coordinate bonds.[101] Reproduced from ref. 100 with permission from Royal Society of Chemistry, copyright 2019. Reproduced from ref. 101 with permission from American Chemical Society, copyright 2019.

retards the disulfide exchange reaction and hence the healing efficiency. Further, an increase in the exposure time of the cut surfaces to the open atmosphere results in a decrease in the healing efficiency of the mended samples.

Epoxidized polyisoprene (epoxidized natural rubber, ENR) contains two reactive functional moieties (epoxy group and unsaturated double bond) and can be easily modified with various crosslinkers and organic molecules to develop self-healing ENR. Imbernon *et al.*[106] introduced disulfide functionality into the ENR using dithiodibutyric acid (DTDB) as a crosslinker (Fig. 17a). DTDB-cured ENR exhibits strong elastomeric properties and behaves like a standard natural rubber until 100 °C. The disulfide exchange reaction makes DTDB-cured ENR reprocessable when heated above 150 °C. After adhering two specimens for 30 min at 180 °C, ENR with disulfide bond (DTDB-cured ENR) shows superior lap-shear strength (20 N) than that without the disulfide bond (5 N). The incorporation of both disulfide functionality and hydrogen bonding into ENR can further improve the self-healing property. Cheng *et al.*[107] prepared a dual cross-linked self-healing ENR based on dynamic disulfide metathesis and thermoreversible hydrogen bonding (Fig. 17b). Two aromatic disulfides (Dithiodibenzoic acid, DTSA, and 4,4′-dithiodianiline, DTDA) along with sulfur (S) are used to improve the self-healing property. The increase in the sulfur content in the DSTA/DDTA/S curing system reduces the healing efficiency as it results in the formation of more permanent crosslinks, which reduce the mobility of the polymer chains. The presence of carbonyl, epoxy, and hydroxyl groups in the dual crosslinked system results in the formation of thermoreversible hydrogen bonds, which further helps in the improvement of mechanical and self-healing properties. The dual cross-linked ENR exhibits good self-healing efficiency (up to 98%) when healed at 120 °C for 24 h.

5.5. Self-healing nanocomposites of epoxy-functionalized IR

The introduction of suitable nanofillers into the ENR can also induce the self-healing property in the nanocomposites. Nie *et al.*[108] and Chen *et al.*[109] studied the self-healing property of ENR/chitin nanocrystals (ENR/CNCs) composites where the supramolecular networks are formed through hydrogen bonding between the CNCs and the epoxy groups of ENR. The supramolecular network improves the mechanical properties and induces the self-healing property in the composite. With 20 wt% CNCs loading, the tensile strength of the ENR/CNCs composites increases twice that of the original strength of neat ENR. The ENR/CNCs composite with 20 wt% filler loading shows good self-healing efficiency (83%). The healing behavior is strongly affected by the CNCs contents, healing temperature, and healing time. Nie *et al.*[110] further studied the effect of the combination of various fillers on the self-healing and mechanical properties of the ENR composites. They dispersed the chitin nanocrystals (CNCs), carboxymethyl chitosan (CMCS), and carboxyl functional multi-walled carbon nanotube (CNT) into ENR in the latex state. The formation of multiple hydrogen bonds between the functional groups of the fillers and

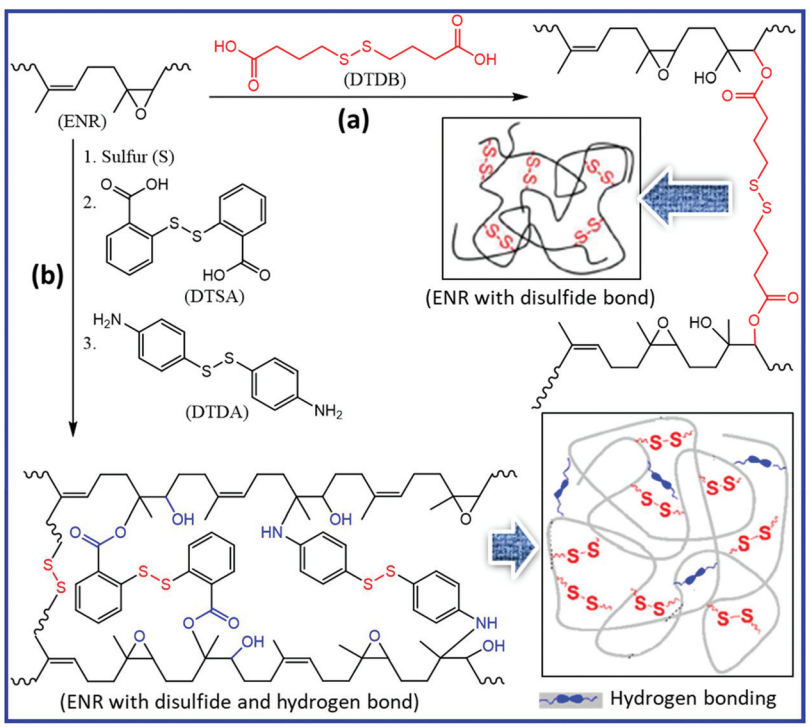

Fig. 17 (a) Schematic representation of the preparation of self-healing ENR having aliphatic disulfide functionality.[106] (b) Self-healing ENR having aromatic disulfide functionality and hydrogen bonding.[107] Reproduced from ref. 106 with permission from Royal Society of Chemistry, copyright 2015. Reproduced from ref. 107 with permission from American Chemical Society, copyright 2019.

ENR result in a healing efficiency of 91%. Interestingly, the tensile strength, as well as the elongation at break of the ENR/CNCs/CMCS/CNT composite, is much higher than that of the pristine ENR.

Cao *et al.*[111] prepared the self-healing nanocomposites based on the ENR/cellulose nanocrystals *via* the dispersion of cellulose nanocrystals in ENR in the latex state. The formation of supramolecular networks *via* dynamic hydrogen bond between the epoxy oxygen of ENR and hydroxyl groups on the cellulose nanocrystals induces the self-healing property in the composite. Supramolecular hydrogen bonding also improves the mechanical property of the composite. The self-healing property is strongly affected by the cellulose nanocrystals' content and healing time. Cao *et al.*[112] further reported the preparation of recyclable and self-healable elastomers composites based on ENR and TOCNs (TEMPO-oxidized cellulose nanocrystals) having a large number of surface carboxyl groups (Fig. 18). The formation of interfacial ester bonds by the reaction between the carboxyl groups of TOCNs and the epoxy groups of ENR results in a covalently crosslinked network structure, which improves the mechanical property of the composite. Interestingly, the network with exchangeable β-hydroxyl ester bonds at the ENR-TOCN interface can change the network topology *via* the transesterification reactions. This transesterification reaction plays an important role in the recycling and self-healing process and results in a healing efficiency of ~80%.

Other fillers such as silica and graphene oxide (having –OH functionality) can induce the self-healing property *via* the formation of hydrogen bonding with NR and ENR. Sattar *et al.*[113] reported the preparation of self-healing NR-silica (NR/SiO_2) composites *via* Mg^{2+}-assisted heteroaggregation of NR (bearing proteins and phospholipids) and silica to produce a reversible supramolecular network mainly constructed by ion-dipole, electrostatic, and hydrogen bonding (Fig. 19a). The Mg^{2+} ions interact with the negatively charged colloids of NR and SiO_2

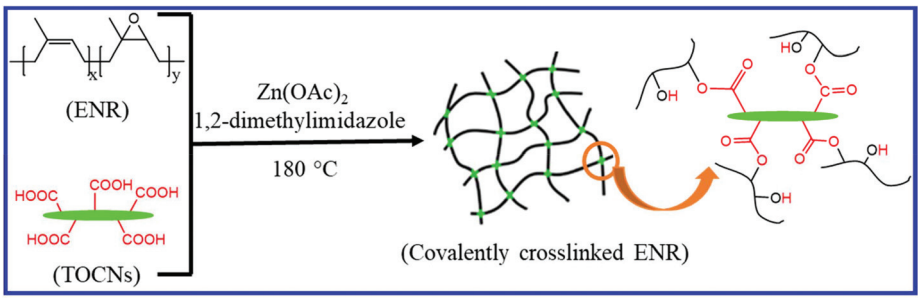

Fig. 18 Schematic representation of the preparation of TOCNs cross-linked ENR *via* the epoxy-acid reaction[112] Reproduced from ref. 112 with permission from Royal Society of Chemistry, copyright 2019.

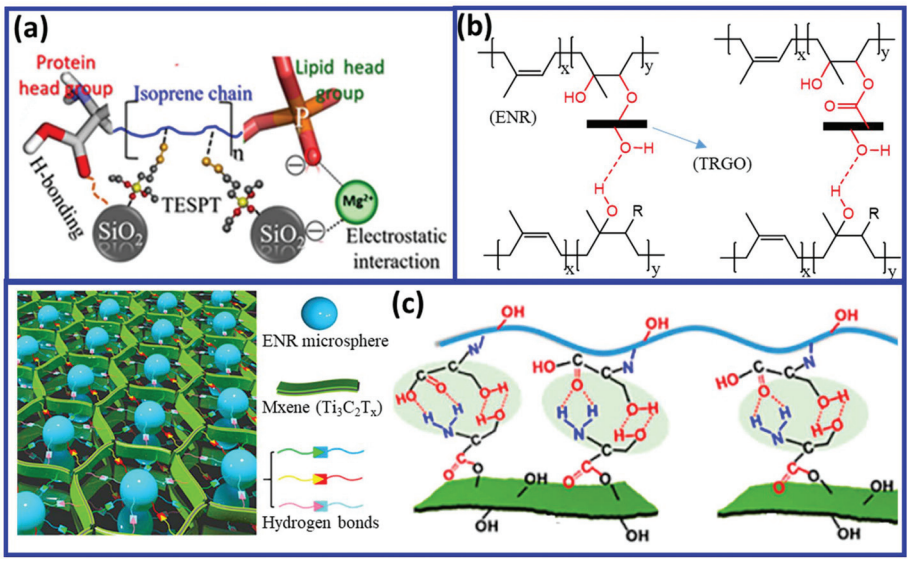

Fig. 19 (a) Schematic representation of the electrostatic interaction and hydrogen bonding in the NR/SiO_2 composites.[113] (b and c) Hydrogen bonding in the ENR/TRGO and serine-modified ENR/Mxene composites.[114,115] Reproduced from ref. 113 with permission from American Chemical Society, copyright 2019. Reproduced from ref. 114 with permission from American Chemical Society, copyright 2020. Reproduced from ref. 115 with permission from American Chemical Society, copyright 2020.

particles and drive the mutual assembly *via* reversible electrostatic interaction and hydrogen bonding. The hydrogen bond is formed between the silanol groups on the silica surface and the lipid groups of NR. The combination of hydrogen bonding and ionic interaction in the NR-silica composites result in the self-healing property. Interestingly, the NR/SiO_2 composites prepared *via* the wet compounding method (mixing in latex state) possess higher healing efficiency (79%) than that prepared *via* the dry mixing process (51.6%). Utrera-Barrios *et al.*[114] prepared self-healing composites based on ENR and thermally-reduced graphene oxide (TRGO) having surface functional groups (hydroxyl, carboxyl, and epoxy) (Fig. 19b). During vulcanization, the hydroxyl and carboxyl group of TRGO reacts with the epoxy group of ENR, which generates covalent linkage (C–O–C) between the TRGO and ENR, which provides good mechanical properties. The ring-opening of the epoxide also generates the –OH functionality in ENR. The –OH and epoxy functionality of ENR are involved in the formation of reversible hydrogen bonding with the functional group of TRGO, which induces the self-healing property in the ENR/TRGO composite. Guo *et al.*[115] developed a self-healing composite by incorporating serine-modified Ti_3C_2MXenes (s-MXenes) into serine-modified ENR (s-ENR) (Fig. 19c). The supramolecular hydrogen bonding interfaces between the s-MXenes and s-ENR results in excellent self-healing property with a healing efficiency of 99.3% after healing at room temperature for 90 min.

Various mechanisms such as DA-rDA reaction, ionic interaction, reversible coordination, hydrogen bonding, disulfide metathesis, and transesterification have been utilized to prepare self-healing IR. Self-healing IR based on transesterification needs very high temperature (160 °C) to show the self-healing property, whereas the DA-rDA-based system exhibits self-healing property at 130 °C. The DA-rDA-based IR further needs to be maintained at 40 °C for a longer time to achieve suitable mechanical property through the formation of DA adducts. Thus, compared to the transesterification reaction, the DA-rDA-based system needs more time to show better healing efficiency. IR based on ionic interaction, reversible coordination, hydrogen bonding, and disulfide metathesis exhibits self-healing property in between 25 °C to 120 °C. Different functional fillers like chitin nanocrystals (CNC), carboxymethyl chitosan (CMCS), carboxyl functional multi-walled carbon nanotube (CNT), cellulose nanocrystals, silica, thermally-reduced graphene oxide (TRGO), and serine-modified Ti_3C_2MXenes have been explored to develop self-healing ENR composites *via* H-bonding. Serine-modified ENR/Ti_3C_2MXene composite shows superior self-healing property over the ENR/CNC, ENR/CMCS, ENR/CNT, and ENR/TRGO composites.

6. Self-healing isoprene isobutyl rubber (butyl rubber, IIR)

Butyl rubber is a random copolymer of isobutylene and isoprene, which contains 1–3% of isoprene units.[116] The presence of the double bond and the methyl group in the isoprene unit make the IIR suitable for various modification and cross-linking processes. Bromobutyl rubber (BIIR) is an important grade of IIR, which is prepared *via* the bromination of IIR.[117,118] The allylic bromide unit in BIIR can be easily modified with amine, phosphine, and imidazole derivatives to form ionomers.[119–124]

6.1. Self-healing IIR *via* ionic interaction and hydrogen bonding

The introduction of ionic moieties is an important way to convert commercial IIR to a self-healing material.[125] Das *et al.*[126] reported the self-healing property of ionomeric butyl rubber (IIIR) prepared by the modification of bromobutyl rubber (BIIR) with butylimidazole. The reaction between the allyl bromide group of BIIR with butylimidazole results in the formation of ionic imidazolium groups having associated bromide anion. The interaction between the imidazolium ionic moieties results in the formation of reversible ionic associates those act as physical crosslinks (Fig. 20a). These ionic association break with an increase in the temperature and again, the association of ionic moieties takes place with a

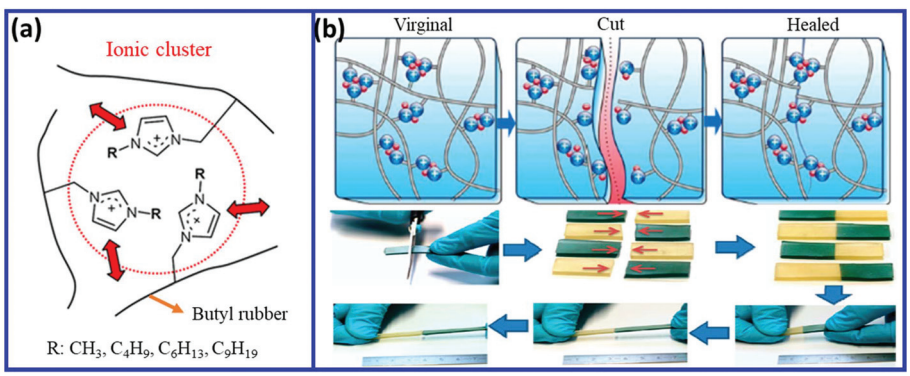

Fig. 20 (a) Schematic representation of the formation of the ionic cluster in the imidazole-modified BIIR.[127] (b) Dissociation and association ionic groups during the self-healing process.[126] Reproduced from ref. 126 with permission from American Chemical Society, copyright 2015. Reproduced from ref. 127 with permission from American Chemical Society, copyright 2017.

further reduction in the temperature. The association, dissociation, and rearrangement of the ionic groups induce the self-healing property in the rubber (Fig. 20b). The ionically-modified BIIR shows superior mechanical properties (elastic modulus, tensile strength, ductility, and hysteresis loss) over those of conventionally sulfur-cured BIIR. The structure of the alkyl imidazole (modifier) also has a great impact on the self-healing property of BIIR. Suckow *et al.*[127] studied the effect of various alkyl imidazole such as 1-methylimidazole, 1-butylimidazole, 1-hexylimidazole, 1-nonylimidazole, and 1-(6-chlorohexyl)-1*H*-imidazole on the self-healing property of ionically-modified BIIR. The self-healing property mainly depends on the nature of the ionic cluster. The strong ionic cluster reduces the chain dynamics, which in turn improves the mechanical properties but reduces the self-healing efficiency. Imidazole with short aliphatic substituents (1-methylimidazole) forms strong clusters and results in poor self-healing property, whereas imidazole with medium alkyl chain length (*e.g.* butyl, hexyl, and nonyl) reduces the cluster strength and improves the chain dynamics and hence the self-healing efficiency. The weaker cluster strength results in poor mechanical properties. Thus, a balance between the mechanical or self-healing property is needed to get the optimum value of both. BIIR modified with 1-hexylimidazole shows the optimum properties with a healing efficiency of 74% (based on the tensile strength) and 98% (based on the elongation at break) and tensile strength and elongation at break of 10.7 MPa and 1040%, respectively. Mordvinkin *et al.*[128] reported that imidazole (methyl-, butyl-, hexyl, or nonylimidazole)-modified BIIR form ionic clusters of about 20 ionic groups. This indicates that the overall structure is governed by the spacing of the ionic groups along the chain and by their strong aggregation tendency in all the cases. The fraction of free ionic groups is small in all the imidazole-modified BIIR. The amplitude of the internal motion of the ionic clusters increases with an increase in the length of the alkyl group of alkylimidazolium.

Stein *et al.*[129] studied the effect of the combination of ionic cluster and hydrogen bonding on the self-healing and reprocessability of bromobutyl rubber. In this case, BIIR is reacted with modifiers having one uracil and one imidazole moiety. The reaction of the allyl bromide units of BIIR with the imidazole moiety results in the formation of imidazolium bromide units (ionic groups), which undergo association to form ionic clusters. The supramolecular physical crosslink is formed *via* triple hydrogen bonding between the uracil groups with a bifunctional linker having two diamidopyridyl moieties. The presence of dual dynamic crosslinks does not help to show the improved self-healing property and the healing efficiency is lower than that of the hexyl imidazole-based ionomer.

6.2. Self-healing IIR-ionomer nanocomposites

The addition of the filler also affects the self-healing property of the ionically-modified BIIR.[130] Le *et al.*[131,132] reported the preparation of self-healing butyl rubber (IIR) by the modification of bromobutyl (BIIR) with imidazole. Further, they loaded the imidazole-modified BIIR with carbon nanotubes (CNTs) to reinforce the matrix and to induce the electrical conductivity. The cation–π interaction between the imidazolium group of butyl rubber and the CNT improves the rubber-CNT interaction and results in better mechanical performance and higher electrical conductivity. The electrically conductive nature of the composite helps to accelerate the healing process just by applying an electrical current across the damaged surface. Sallat *et al.*[133] studied the effect of addition of silica nanoparticles on the self-healing and mechanical properties of ionically-modified BIIR (modified using 1-butylimidazole). In addition to pristine (precipitated) silica, they also used silanized silica nanoparticles with aliphatic or imidazolium functional groups. The interaction between the ionic group of ionically-modified BIIR and the functional groups of silica nanoparticles strongly improves the mechanical properties but with a reduction in the self-healing efficiency. The tensile strength of ionically-modified BIIR is 10.2 MPa and increased to 12 MPa, 18.9 MPa, and 18.9 MPa, respectively, due to its composites with pristine, alkyl-functionalized, and imidazolium-functionalized silica nanoparticles. No improvement in the tensile strength is observed when the modification of silica is performed *via* the *in situ* process during compounding. This may be because of the presence of unreacted modifier molecules that are not successfully grafted over the silica nanoparticles. The pristine ionically-modified BIIR shows a healing efficiency of 87 ± 50%, which reduces to 32–43% for its silica nanocomposites. Interestingly, the tensile stress and elongation at break of the composites after healing are comparable with those of the pristine ionomer.

Most of the reported literature on self-healing BIIR is based on imidazolium-based ionic moiety. Phosphonium, ammonium, and pyridinium based ionic groups can also be incorporated into BIIR *via* reaction with phosphine, amine, and pyridine-based nucleophiles. The effect of the phosphonium, ammonium, and pyridinium-based ionic moieties on the self-healing property of BIIR should be evaluated and compared with the imidazolium-based ionic moiety.

7. Self-healing nitrile butadiene rubber (NBR)

7.1. Self-healing NBR based on coordination bond

NBR contains a double bond as well as a nitrile functionality. The nitrile group in NBR acts as a ligand and forms complexes with metal salts. Nitrile rubber is also crosslinked using metal salts, where the crosslinks are formed *via* the coordination reaction between the nitrile group and the metal atom.[134] If the coordination bond between the nitrile group and the metal is reversible, then the coordination crosslinked NBR can be easily reprocessed. The functional group of the functionalized NBR can also be utilized to form a reversible coordinate bond with suitable metal ions. Cheng *et al.*[135] reported the preparation of recyclable NBR by the functionalization of epoxidized NBR with dopamine, followed by the formation of coordination crosslinks between the catechol groups of dop-

amine and Fe^{3+} ion. The introduction of crosslinks *via* reversible coordination chemistry can also induce the self-healing property in NBR. Zhang *et al.*[136] reported the preparation of self-healable and reprocessable coordination-crosslinked NBR using cobalt neocaprate (cobalt(II) decanoate) as a crosslinker (Fig. 21). When the healing is performed at 190 °C for 10 min, the coordination-crosslinked NBR shows a healing efficiency of 72%, whereas it is only 26% in sulfur-crosslinked NBR. NBR loaded with 30 phr of cobalt neocaprate exhibits superior tensile strength and higher elongation at break than that of the sulfur (1.5 phr)-cured NBR sample. The cobalt neocaprate-crosslinked NBR exhibits higher modulus and tensile strength after recycling. The nature of the metal–ligand bond also has a strong influence on the self-healing efficiency. Das *et al.*[137] studied the effect of various metal salts (Co^{+2}, Ni^{+2}, and Zn^{+2} based metal salts) on the self-healing property of 2,6-diaminopyridine-functionalized carboxylated nitrile butadiene rubber (DAP-XNBR). Zn^{+2}-coordinated DAP-XNBR exhibits better self-healing efficiency than that of Co^{+2} and Ni^{+2}, whereas the tensile strength of the Co^{+2} and Ni^{+2}-coordinated DAP-XNBR is much higher than that of Zn^{+2}. The higher healing efficiency in Zn^{+2} coordinated DAP-XNBR is due to the dynamic nature of the metal–ligand bond, whereas the stronger metal–ligand bond in Ni^{+2}-coordinated DAP-XNBR reduces the healing efficiency. The healing efficiency Co^{+2}, Ni^{+2}, and Zn^{+2}-coordinated DAP-XNBR increases with an increase in the healing temperature.

7.2. Self-healing NBR *via* blending with other polymers

NBR can also be made self-healable by blending with suitable polymeric materials. Schüssele *et al.*[138] studied the self-healing property of NBR by blending with hyperbranched polyethyleneimine and their urea derivatives. Neat NBR shows a healing efficiency of 4% when the cut samples are healed at 100 °C for 12 h. However, the blending of 12 phr of hyperbranched polyethyleneimine (PEI) with NBR results in a healing efficiency of 27–44%. The blending of high molecular weight PEI (2000 g mol^{-1}) with NBR shows better healing efficiency (44%) than that of low molecular weight PEI (800 g mol^{-1}). The blending of poly(acrylic acid)-grafted ground tire rubber (PAA-g-GTR) also has a great impact on the self-healing property of NBR. Barrios *et al.*[139] compared the self-healing property of the XNBR/ZnO compound with the PAA-g-GTR-added XNBR/ZnO (XNBR/ZnO/PAA-g-GTR). In XNBR/ZnO, Zn^{2+} form ionic crosslinks with the acid group of XNBR, and the association and dissociation of ionic groups results in the self-healing property. The addition of PAA-g-GTR into the XNBR/ZnO compound further improves the healing efficiency, which is due to the formation of additional ionic clusters *via* interaction between the acid groups of PAA-g-GTR and Zn^{2+}. The healing efficiency of the XNBR/ZnO compound is 15%, which increased to 70% for the XNBR-ZnO-PAA-g-GTR compound. NBR as an additive also improves the self-healing efficiency of other self-healing polymeric systems. Feng *et al.*[140] reported that the self-healing efficiency of epoxy resins (based on the Diels–Alder reaction) can be improved by introducing NBR into it. The blending of 0, 5, 10, and 15 phr of NBR to the self-healing epoxy system results in a healing efficiency of 70.0%, 81.5%, 84.9%, and 88.6%, respectively.

7.3. Self-healing NBR *via* DA/rDA reaction and disulfide metathesis reaction

The self-healing property of NBR can be improved *via* the introduction of dual dynamic covalent bonds. Sarkar *et al.*[141] reported the preparation of self-healing XNBR based on dynamic photo-triggered disulfide metathesis and thermoreversible Diels–Alder (DA) "click" chemistry (Fig. 22). They first prepared a furan-functionalized XNBR (FXNBR) *via* the reaction of XNBR with furfuryl amine, followed by crosslinking with a dual functional crosslinker (BMDS) having maleimide as well as disulfide functionalities that can participate in the DA reaction and disulfide metathesis reaction. The BM-DS crosslinked FXNBR (FXNBR-BMDS) shows a healing efficiency of 60–91% when healed at 125 °C for 4 h, followed by cooling down to RT, and this temperature was maintained for another 12 h. The increased BM-DS content in the FXNBR-BMDS results in an increase in the tensile strength but reduces the self-healing efficiency. The improved tensile strength is due to

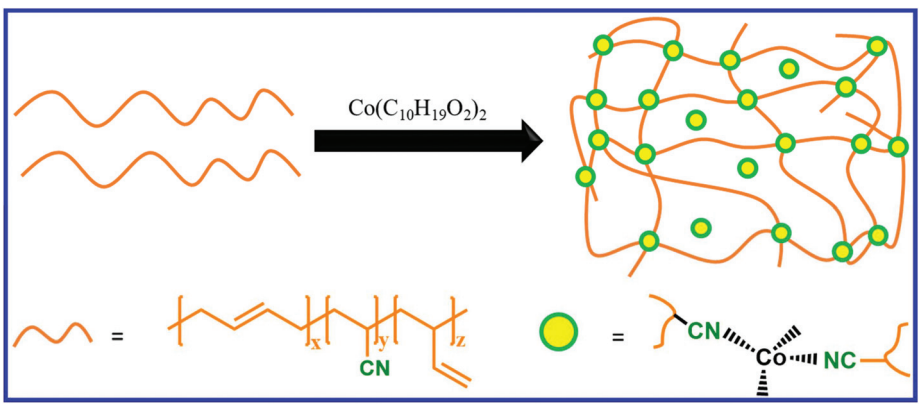

Fig. 21 Schematic representation of the preparation of coordination crosslinked NBR.[136]

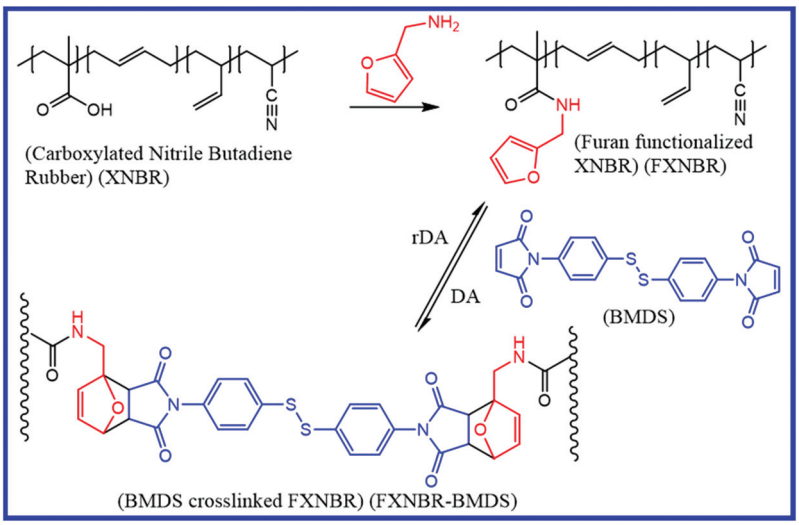

Fig. 22 Schematic representation of the preparation of self-healing XNBR having disulfide moiety and DA bond.[141]

the increase in the crosslink density, which in turn reduces the chain mobility and self-healing efficiency. The FXNBR-BMDS also shows self-healing property under UV irradiation (for 4 h), which is due to the disulfide metathesis reaction. The FXNBR-BMDS sample with similar BMDS content (furan : BMDS = 1 : 0.07) shows a healing efficiency of 74% and 78% under thermal and UV irradiation, respectively. The authors studied the individual effect of thermal and UV irradiation on the self-healing property. The study of the effect of a combined dose of thermal and UV irradiation on the self-healing property would have been more interesting.

8. Self-healing chloroprene rubber (CR)

Sulfur-crosslinked CR can be made self-healable and reprocessable by the incorporation of a suitable catalyst that can cause a disulfide metathesis reaction. Xiang *et al.*[142] reported the use of organic complex copper(II) methacrylate (MA-Cu) as a novel catalyst to trigger disulfide metathesis at elevated temperatures. When the catalyst is incorporated into the vulcanized CR, the reshuffling of inherent sulfur crosslinks is enabled

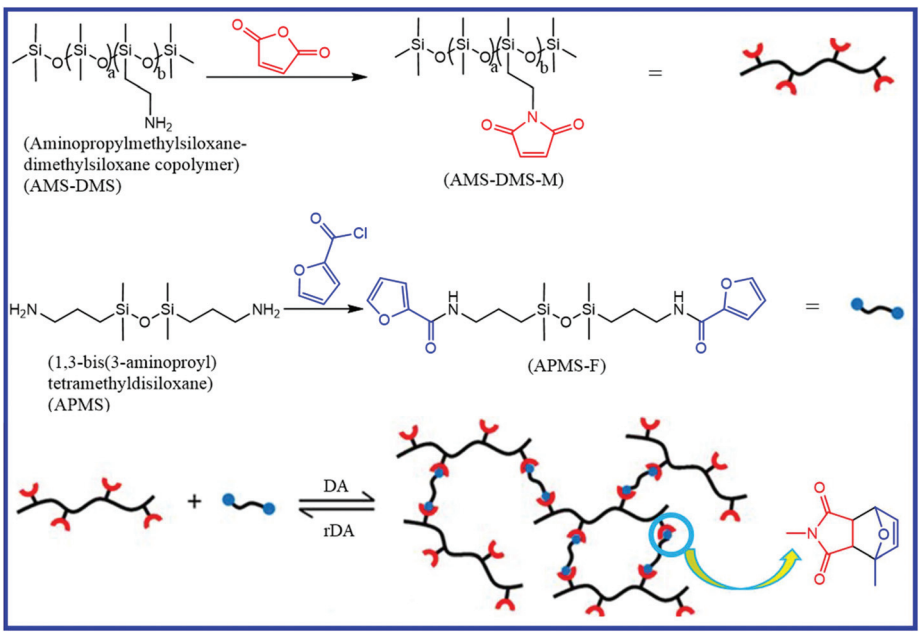

Fig. 23 Schematic representation of the preparation of the self-healing polysiloxane elastomer with DA bonds.[155] Reproduced from ref. 155 with permission from Royal Society of Chemistry, copyright 2016.

typically at 120 °C, while the microstructure of the material remains unchanged at a lower temperature (typically lower than 100 °C). The presence of the catalyst activates the disulfide bond, as a result of which the sulfur bonds are reversibly exchanged inside the vulcanized chloroprene rubber as well as across the surfaces at 120 °C. The exchange of disulfide

Table 1 Rubber composition, self-healing mechanism, healing conditions, and self-healing efficiency

Rubber/modified rubber/other chemicals	Healing mechanism	Healing conditions	Healing efficiency (%)	Recyclability	Ref.
Furan functionalized PB & bismaleimide	DA & rDA	—	—	Recyclable at 110 °C	68
Furan functionalized PB & bismaleimide	DA & rDA	150 °C & 60 °C	—	Recyclable at 160 °C	69
PB/polysulfide	Disulfide metathesis	UV irradiation	93–97	Recyclable under UV light	71
S-crosslinked PB/$CuCl_2$	Disulfide exchange	110 °C 12 h	75	Recyclable at 110 °C	72
PB oligomers having carboxylic acid and amine groups/tri-thiol crosslinker	Ionic hydrogen bonds	RT, 1 h	33–93	—	73
PB/1*H*,1*H*,2*H*,2*H*-perfluorodecanethiol	Crystallite melting	80 °C	—	—	75
XSBR/NCS composites (NCS 20 wt%)	Supramolecular hybrid network	RT, 24 h	92	—	80
Furan functionalized SBR/MWCNT & bismaleimide	DA & rDA	100 °C, 5 h	90	Recyclable at 130–150 °C	81
Furan functionalized NR & bismaleimide	DA & rDA	100 °C, 4 h & 40 °C, 3–7 h	38–85	Recyclable	85
Carboxylated IR & NaOH	Ionic interaction	28 °C	80	—	86
NR/methacrylic acid/ZnO	Ionic interaction	RT, 20 min	96–100	—	91
Dopamine modified ENR/Fe^{3+}	Reversible coordinate bond	50 °C, 12–24 h	89–93	—	96
ZnCl-decorated ENR/histidine modified CNC	Reversible coordinate bond	RT, 2 min	107	—	97
Maleic anhydride grafted NR/ 3-amino-1,2,4-triazole/$ZnCl_2$	Hydrogen bond & reversible coordinate bond	80 °C, 12–24 h	74	—	100
ENR/dithiol-bearing boronic ester/ $ZnCl_2$	boronic ester transesterifications & reversible coordinate bond	80 °C, 24 h	60–100	Recyclable at 160 °C	101
NR/S/accelerator (CBS) a/s = 0.2	Disulfide exchange	70 °C, 7 h	3–80	—	105
ENR/dithiodibenzoic acid/4,4′-dithiodianiline/S	Disulfide metathesis and hydrogen bonding	120 °C, 5 h	98	Recyclable at 155 °C	107
ENR/chitin nanocrystals (20 phr)	Hydrogen bonding	RT, 24 h	83	—	108
ENR/cellulose nanocrystals (20 phr)	Hydrogen bonding	RT, 24 h	86	—	111
ENR/TEMPO-oxidized cellulose nanocrystals	Transesterification reaction	160 °C, 3 h	80	Recyclable at 160 °C	112
NR/SiO_2/$MgSO_4$ (activator and sulfur curing agents)	Hydrogen bonding and ionic interaction	50 °C, 24 h	51–79	—	114
Serine modified Ti_3C_2MXenes/ serine modified ENR	Hydrogen bonding	RT, 90 min	99.3	—	115
BIIR/1-butylimidazole	Ionic interaction	RT–100 °C, 1–192 h	—	Recyclable in solvent or above 130 °C	126
BIIR/1-methylimidazole	Ionic interaction	70 °C, 16 h (pressed together with a compression of 0.1 mm)	18 ± 13		127
BIIR/1-butylimidazole			25 ± 16		
BIIR/1-hexylimidazole			74 ± 43		
BIIR/1-nonylimidazole			57 ± 39		
BIIR/1-butylimidazole	Ionic interaction and acid–base interaction	70 °C, 16 h (under slight pressure)	87 ± 50		133
BIIR/1-butylimidazole/pristine silica			40 ± 25		
BIIR/1-butylimidazole/alkyl functionalized silica			43 ± 23		
BIIR/1-butylimidazole/imidazolium functionalized silica			32 ± 16		
NBR/cobalt neocaprate	Coordination	190 °C, 10 min	72	Recyclable	136
NBR/sulfur	—		26	—	
NBR		100 °C, 12 h	4	—	138
NBR/PEI			27–44	—	
Furan functionalized NBR & bismaleimide with disulfide moiety	DA, rDA and Disulfide metathesis	125 °C for 4 h, cooling down to RT and held for 12 h	60–75–91	Recyclable at 130 °C	141
		UV irradiation for 4 h	78		
Furan and maleimide functionalized polysiloxane	DA & rDA	140 °C for 3 h and 80 °C for 1–24 h	29–95	Recyclable at 140 °C	155

bonds *via* the metathesis reaction results in repeated reshaping, self-healing, and recycling of the crosslinked CR. The disulfide metathesis reaction is only possible for disulfide and polysulfide linkages. However, the formation of more monosulfide linkages during vulcanization may act as permanent crosslinks and retard the self-healing process.

9. Self-healing diene-functionalized silicone rubber

Silicone rubber (polysiloxane) differs from other elastomers in the structure of its backbone, which consists of Si–O–Si units. The wide applications of silicone rubber in biomedical devices and seals have attracted significant attention for the development of self-healing silicone rubber that can improve the application life. Besides a large number of pieces of literature on self-healing silicone rubber,[143–154] only a few have been reported on the field of diene-functionalized self-healing silicone rubber. Zhao *et al.*[155] reported a healable polysiloxane elastomer *via* the crosslinking of polydimethylsiloxane-bearing maleimide pendants (AMS-DMAS-M) with furan–end functionalized siloxane (APMS-F) *via* the Diels–Alder (DA) reaction (Fig. 23). For comparison purposes, they also prepared a crosslinked polysiloxane sample without the DA bonds. The DA-crosslinked polysiloxane elastomers show the self-healing property for thermal treatment at 140 °C for 3 h and at 80 °C for different times. At 140 °C, the cleavage of the crosslinks (DA adduct) takes place *via* retro Diels–Alder reaction, which generates the furan (diene) and maleimide (dienophile) functionality on the polysiloxane elastomers. These furan and maleimide groups are again recombined at 80 °C and result in the formation of DA crosslinks. The increase in the thermal treatment time at 80 °C results in an increase in the healing efficiency, which is due to the formation of more crosslinks *via* the DA reaction. DA-crosslinked polysiloxane elastomers show a healing efficiency of 29%, 59%, 89%, and 95% on respective thermal treatment for 1 h, 6 h, 12 h, and 24 h at 80 °C. The content of DA adducts and the molecular weight of the polysiloxane elastomer has a strong impact on the self-healing efficiency. An increase in the content of DA adducts and a decrease in the molecular weight of the polysiloxane elastomer results in an improvement in the healing efficiency. The higher healing efficiency of the low molecular weight polysiloxane elastomer is due to the better chain mobility than that of the high molecular weight counterpart. Interestingly, the DA-crosslinked polysiloxane elastomer shows similar healing efficiency even after remolding *via* hot compression at 140 °C (for 1.5 h under a pressure of 20 MPa), followed by cooling down to 80 °C and remaining at this temperature for 24 h. This indicates that the DA-crosslinked polysiloxane elastomer is reprocessable similar to thermoplastic elastomers. In contrast, the crosslinked polysiloxane sample without DA bonds does not exhibit self-healing and reprocessable properties. The incorporation of nanoparticles into the DA-based self-healing polysiloxane system also affects the mechanical and self-healing properties. Zhao *et al.*[156] studied the effect of graphene nanosheets on self-healable and mechanical properties of polysiloxane/graphene nanocomposites. The pristine DA crosslinked polysiloxane elastomer shows a tensile strength of 0.059 MPa and a self-healing efficiency of >90% (healing condition: 80 °C for 12 h) even after three successive healing cycles. The incorporation of 35 wt% graphene nanosheets results in an 18-fold increase in the tensile strength without compromising the self-healing efficiency.

10. Summary

The mechanism of self-healing, healing efficiency, healing conditions, recyclability, and recyclability conditions of the different diolefin-based elastomeric systems is summarized in Table 1.

11. Conclusions, challenges, and future research opportunities

Diels–Alder reaction, disulfide metathesis reaction, ionic interaction, reversible coordinate bond, and reversible hydrogen bonding are important mechanisms that induce self-healing property in elastomeric materials. Each mechanism has its own merits and demerits. Self-healing elastomers based on the Diels–Alder reaction show good mechanical property but need high temperatures to show self-healing property. Though the Diels–Alder reaction-based self-healing systems are covalently crosslinked, these can be easily reprocessed by heating above the retro Diels–Alder reaction temperature. The disulfide exchange mechanism, ionic interaction, hydrogen bonding, and reversible coordinate bond induce the self-healing property at somewhat lower temperatures (also depend upon the crosslink density and elastomeric system) but do not provide good mechanical properties. Depending on the elastomeric system, the disulfide mechanism shows self-healing property under thermal or UV irradiation or even at room temperature. The longer exposure of the cut surfaces of disulfide-based self-healing elastomers to the open atmosphere reduces the healing efficiency due to the deactivation of the sulfide radicals. In the case of ionically-modified elastomers, the healing efficiency strongly depends on the nature of the ionic moiety. Very weak ionic interaction reduces the healing efficiency and the mechanical properties. The formation of a very strong ionic cluster provides good mechanical properties but reduces the self-healing efficiency. Hence, an optimized ionic interaction is crucial for achieving better self-healing property. The introduction of both permanent and dynamic crosslinks improves the mechanical property but the permanent network reduces the chain dynamics and hence the self-healing property. Thus, it is quite a challenging task to design a self-healing elastomer with good mechanical as well as self-healing properties.

The self-healing elastomers based on multi-dynamic networks need to be explored to achieve excellent self-healing and good mechanical properties. For example, aromatic disulfide, ionic interaction, and DA adducts can be introduced to a single elastomeric system. Aromatic disulfide can show self-healing property at room temperature and the ionic group can be manipulated to show the self-healing property at 60–100 °C; furthermore, the DA adduct will show self-healing property at 120–160 °C. In this kind of multi-mechanism healing system, the healing of micro-cracks will occur at room temperature due to disulfide metathesis reaction, whereas the ionic interaction (physical crosslinks) and DA adducts (covalent crosslinks) will provide good mechanical properties. For a crack of intermediate intensity, the material can be heated above the dissociation temperature of the ionic crosslinks so that the material can heal *via* a dual mechanism, *i.e.*, the involvement of both ionic and disulfide exchange mechanisms. In case of a bigger crack, the elastomer can be heated above the rDA reaction temperature, which will improve the chain mobility and the healing will take place through the combination of disulfide metathesis, reversible ionic interaction, and reversible DA/rDA reaction. Multi-stimuli (heat, light, chemical, mechanical, *etc*.) responsive self-healing elastomers can also be explored by introducing various functional moieties into a single elastomeric system. A detailed study of the individual and combined effects of the stimuli on the self-healing efficiency would be more interesting.

There are few reports in the area of self-healing SBR, which has the single largest synthetic rubber application in the rubber industry. High styrene content SBR or hydrogenated SBR with self-healing property will further expand the application areas of SBR. More work should also be done on the development of self-healing CR, which has not been explored much.

Elastomers are mostly used by compounding with different fillers. Conventional fillers hinder the interaction between the functional groups of the self-healing elastomers, resulting in reduced healing efficiency. Fillers with a suitable functional moiety that can reversibly interact with the functional groups of the self-healing elastomers should be explored to achieve optimum self-healing and mechanical properties. Without in-depth studies of self-healing elastomer composites, commercialization is nearly an impossible target. Hence, maximum effort should be given to the development of self-healing elastomeric composite rather than pristine rubber.

Despite the great efforts in the development of self-healing elastomers, there are serious limitations that need to be resolved. Evaluating the self-healing efficiency through tensile measurement or monitoring superficial cracks is insufficient to ensure the behavior in the service of self-healing elastomeric materials. The impact of external environmental conditions on the self-healing property of the elastomers and elastomer composites also needs to be evaluated for real applications.

Elastomers such as PB, SBR, NR, and IIR are mostly used in the tire industry and always perform under cyclic thermal/mechanical stress. Thus, future research should also be focused on mechano-responsive and thermoresponsive self-healing elastomers that can exhibit self-healing property under mechanical/thermal stress. IIR-based rubbers having self-healing properties will help in puncture-proof tires during the application itself. These special PB/SBR/NR used in tire tread/sidewall will increase the life cycle of the tire. Hence, this self-healing concept development and commercialization will have utmost importance and the need of the hour for next-generation automatic vehicles. The application research of these new materials is to be explored in the automotive segment. Another important upcoming application area of elastomers is in the flexible electronic segment. Electronic items, being costly, a higher life cycle is the most desired. If self-healing elastomers can be used in this area, the life cycle of the products can be enhanced. This will in turn reduce the cost of gadgets as well as the desired reduction in electronic wastes.

The increasing demand for elastomeric materials is resulting in huge elastomeric wastes. This review has described the recent advances in smart elastomeric materials, which could be a potential alternative to reduce the elastomeric waste by extending their application life and making them suitable for reprocessing. We hope that this review will serve as an inspiration for the research community to take this field ahead and to make the sense of self-healing elastomers in real life for a sustainable society.

Conflicts of interest

The authors declare no conflict of interest.

References

1 E. McDonel, K. Baranwal and J. Andries, in *Polymer blends*, Elsevier, 1978, pp. 263–292.
2 D. Barnard, C. Baker and I. Wallace, *Rubber Chem. Technol.*, 1985, **58**, 740–750.
3 B.-K. Kwak, *Elastomers Compos.*, 1974, **9**, 5–13.
4 K. Hashimoto, A. Maeda, K. Hosoya and Y. Todani, *Rubber Chem. Technol.*, 1998, **71**, 449–519.
5 T. S. Mroczkowski, *US Pat.*, 5162409, 1992.
6 H. Schnecko, in *Rubber recycling, Macromolecular Symposia*, Wiley Online Library, 1998, pp. 327–343.
7 B. Adhikari, D. De and S. Maiti, *Prog. Polym. Sci.*, 2000, **25**, 909–948.
8 L. Bockstal, T. Berchem, Q. Schmetz and A. Richel, *J. Cleaner Prod.*, 2019, **236**, 117574.
9 J. E. Morin, D. E. Williams and R. J. Farris, *Rubber Chem. Technol.*, 2002, **75**, 955–968.
10 C. Berrueco, E. Esperanza, F. Mastral, J. Ceamanos and P. García-Bacaicoa, *J. Anal. Appl. Pyrolysis*, 2005, **74**, 245–253.
11 S. Mohanty, P. Mukunda and G. B. Nando, *Polym. Degrad. Stab.*, 1995, **50**, 21–28.

12 L. Imbernon and S. Norvez, *Eur. Polym. J.*, 2016, **82**, 347–376.
13 A. Jones and H. Dutta, *Mech. Mater.*, 2010, **42**, 481–490.
14 H. Ur Rehman, Y. Chen, M. S. Hedenqvist, H. Li, W. Xue, Y. Guo, Y. Guo, H. Duan and H. Liu, *Adv. Funct. Mater.*, 2018, **28**, 1704109.
15 A. M. Wemyss, C. Bowen, C. Plesse, C. Vancaeyzeele, G. T. Nguyen, F. Vidal and C. Wan, *Mater. Sci. Eng., R*, 2020, **141**, 100561.
16 J. L. Wietor and R. P. Sijbesma, *Angew. Chem., Int. Ed.*, 2008, **47**, 8161–8163.
17 S. R. White, B. J. Blaiszik, S. L. Kramer, S. C. Olugebefola, J. S. Moore and N. R. Sottos, *Am. Sci.*, 2011, **99**, 392–399.
18 P. Jacob, P. Kashyap, T. Suparat and C. Visvanathan, *Waste Manage. Res.*, 2014, **32**, 918–926.
19 Z. Bao, J. Tao and C. Flanigan, *Polym. Compos.*, 2017, **38**, 918–926.
20 G. Hermenegildo, E. Bischoff, R. Mauler, M. Giovanela, L. Carli and J. Crespo, *J. Elastomers Plast.*, 2017, **49**, 47–61.
21 T. Shimizu, T. Tsuboi, T. Endo, K. Kobayashi and M. Daitoku, *US Pat.*, 20160311259A1, 2016.
22 S. Mohanty, G. B. Nando, K. Vijayan and N. Neelakanthan, *Polymer*, 1996, **37**, 5387–5394.
23 K. Imato and H. Otsuka, *Dynamic Covalent Chemistry: Principles, Reactions, and Applications*, Wiley Online Library, 2017, pp. 359–387.
24 Y. Yang and M. W. Urban, *Adv. Mater. Interfaces*, 2018, **5**, 1800384.
25 K. Urdl, A. Kandelbauer, W. Kern, U. Müller, M. Thebault and E. Zikulnig-Rusch, *Prog. Org. Coat.*, 2017, **104**, 232–249.
26 S. R. White, N. R. Sottos, P. H. Geubelle, J. S. Moore, M. R. Kessler, S. Sriram, E. N. Brown and S. Viswanathan, *Nature*, 2001, **409**, 794–797.
27 D. Y. Zhu, M. Z. Rong and M. Q. Zhang, *Prog. Polym. Sci.*, 2015, **49**, 175–220.
28 S. An, M. W. Lee, A. L. Yarin and S. S. Yoon, *Chem. Eng. J.*, 2018, **344**, 206–220.
29 S. J. Garcia, *Eur. Polym. J.*, 2014, **53**, 118–125.
30 N. Zhong and W. Post, *Composites, Part A*, 2015, **69**, 226–239.
31 Z. Wang, X. Lu, S. Sun, C. Yu and H. Xia, *J. Mater. Chem. B*, 2019, **7**, 4876–4926.
32 P. Cordier, F. Tournilhac, C. Soulié-Ziakovic and L. Leibler, *Nature*, 2008, **451**, 977–980.
33 F. Herbst, D. Döhler, P. Michael and W. H. Binder, *Macromol. Rapid Commun.*, 2013, **34**, 203–220.
34 N. Duan, Z. Sun, Y. Ren, Z. Liu, L. Liu and F. Yan, *Polym. Chem.*, 2020, **11**, 867–875.
35 P. K. Behera, P. Mondal and N. K. Singha, *Polym. Chem.*, 2018, **9**, 4205–4217.
36 S. L. Banerjee, S. Samanta, S. Sarkar and N. K. Singha, *J. Mater. Chem. B*, 2020, **8**, 226–243.
37 S. Burattini, H. M. Colquhoun, B. W. Greenland and W. Hayes, *Faraday Discuss.*, 2009, **143**, 251–264.
38 S. Burattini, H. M. Colquhoun, J. D. Fox, D. Friedmann, B. W. Greenland, P. J. Harris, W. Hayes, M. E. Mackay and S. J. Rowan, *Chem. Commun.*, 2009, 6717–6719.
39 Z. Wang, C. Xie, C. Yu, G. Fei, Z. Wang and H. Xia, *Macromol. Rapid Commun.*, 2018, **39**, 1700678.
40 M. Nakahata, Y. Takashima and A. Harada, *Macromol. Rapid Commun.*, 2016, **37**, 86–92.
41 X. Chen, M. A. Dam, K. Ono, A. Mal, H. Shen, S. R. Nutt, K. Sheran and F. Wudl, *Science*, 2002, **295**, 1698–1702.
42 A. A. Kavitha and N. K. Singha, *Macromolecules*, 2010, **43**, 3193–3205.
43 N. B. Pramanik, G. B. Nando and N. K. Singha, *Polymer*, 2015, **69**, 349–356.
44 A. A. Kavitha and N. K. Singha, *ACS Appl. Mater. Interfaces*, 2009, **1**, 1427–1436.
45 P. K. Behera, P. Mondal and N. K. Singha, *Macromolecules*, 2018, **51**, 4770–4781.
46 P. Mondal, P. K. Behera, B. Voit, F. Böhme and N. K. Singha, *Macromol. Mater. Eng.*, 2020, 2000142.
47 P. Mondal, G. Jana, P. K. Behera, P. K. Chattaraj and N. K. Singha, *Polym. Chem.*, 2019, **10**, 5070–5079.
48 S. Banerjee, B. V. Tawade and B. Améduri, *Polym. Chem.*, 2019, **10**, 1993–1997.
49 S. K. Raut, P. K. Behera, T. S. Pal, P. Mondal, K. Naskar and N. K. Singha, *Chem. Commun.*, 2021, **57**, 1149–1152.
50 P. Mondal, P. K. Behera and N. K. Singha, *Chem. Commun.*, 2017, **53**, 8715–8718.
51 P. Mondal, P. K. Behera and N. K. Singha, *Prog. Polym. Sci.*, 2021, **113**, 101343.
52 P. Mondal, G. Jana, P. K. Behera, P. K. Chattaraj and N. K. Singha, *Macromolecules*, 2020, **53**, 8313–8323.
53 C.-M. Chung, Y.-S. Roh, S.-Y. Cho and J.-G. Kim, *Chem. Mater.*, 2004, **16**, 3982–3984.
54 S. Banerjee, R. Tripathy, D. Cozzens, T. Nagy, S. Keki, M. Zsuga and R. Faust, *ACS Appl. Mater. Interfaces*, 2015, **7**, 2064–2072.
55 M. Bag, S. Banerjee, R. Faust and D. Venkataraman, *Sol. Energy Mater. Sol. Cells*, 2016, **145**, 418–422.
56 A. Rekondo, R. Martin, A. R. de Luzuriaga, G. Cabañero, H. J. Grande and I. Odriozola, *Mater. Horiz.*, 2014, **1**, 237–240.
57 R. Martin, A. Rekondo, A. R. de Luzuriaga, G. Cabañero, H. J. Grande and I. Odriozola, *J. Mater. Chem. A*, 2014, **2**, 5710–5715.
58 P. K. Behera, S. K. Raut, P. Mondal, S. Sarkar and N. K. Singha, *ACS Appl. Polym. Mater.*, 2021, **3**, 847–856.
59 C. Kim, H. Ejima and N. Yoshie, *J. Mater. Chem. A*, 2018, **6**, 19643–19652.
60 C.-H. Li, C. Wang, C. Keplinger, J.-L. Zuo, L. Jin, Y. Sun, P. Zheng, Y. Cao, F. Lissel and C. Linder, *Nat. Chem.*, 2016, **8**, 618–624.
61 B. Jony, M. Thapa, S. Mulani and S. Roy, In Proceedings of the American Society for Composites—Thirty-third Technical Conference, 2018.
62 S. García, H. Fischer and S. Van Der Zwaag, *Prog. Org. Coat.*, 2011, **72**, 211–221.

63 L. Dai, X. Wang, Z. Bu, B. G. Li and S. Jie, *J. Appl. Polym. Sci.*, 2019, **136**, 46934.
64 C. M. Geiselhart, J. T. Offenloch, H. Mutlu and C. Barner-Kowollik, *ACS Macro Lett.*, 2016, **5**, 1146–1151.
65 L. Xu, B.-G. Li, S. Jie, Z. Li and Z. Bu, *Ind. Eng. Chem. Res.*, 2019, **58**, 13085–13092.
66 P. K. Behera, P. Mandal, M. Maiti, R. V. Jasra and N. K. Singha, *Rubber Chem. Technol.*, 2016, **89**, 335–348.
67 O. Türünç and M. A. Meier, *Macromol. Rapid Commun.*, 2010, **31**, 1822–1826.
68 E. Trovatti, T. M. Lacerda, A. J. Carvalho and A. Gandini, *Adv. Mater.*, 2015, **27**, 2242–2245.
69 J. Bai, H. Li, Z. Shi and J. Yin, *Macromolecules*, 2015, **48**, 3539–3546.
70 P. Berto, A. Pointet, C. Le Coz, S. Grelier and F. Peruch, *Macromolecules*, 2018, **51**, 651–659.
71 H. Xiang, J. Yin, G. Lin, X. Liu, M. Rong and M. Zhang, *Chem. Eng. J.*, 2019, **358**, 878–890.
72 H. Xiang, H. Qian, Z. Lu, M. Rong and M. Zhang, *Green Chem.*, 2015, **17**, 4315–4325.
73 D. Wang, J. Guo, H. Zhang, B. Cheng, H. Shen, N. Zhao and J. Xu, *J. Mater. Chem. A*, 2015, **3**, 12864–12872.
74 R. Jasra, M. Maiti and V. Srivastava, *US Pat.*, 20150045496A1, 2015.
75 F. Xu, X. Li, D. Weng, Y. Li and J. Sun, *J. Mater. Chem. A*, 2019, **7**, 2812–2820.
76 A. F. Halasa, J. Prentis, B. Hsu and C. Jasiunas, *Polymer*, 2005, **46**, 4166–4174.
77 M. Alimardani and F. Abbassi-Sourki, *J. Compos. Mater.*, 2015, **49**, 1267–1282.
78 S. Mukhopadhyay, P. Sahu, H. Bhajiwala, S. Mohanty, V. Gupta and A. K. Bhowmick, *J. Mater. Sci.*, 2019, **54**, 14986–14999.
79 C. Xu, X. Huang, C. Li, Y. Chen, B. Lin and X. Liang, *ACS Sustainable Chem. Eng.*, 2016, **4**, 6981–6990.
80 C. Xu, J. Nie, W. Wu, L. Fu and B. Lin, *Carbohydr. Polym.*, 2019, **205**, 410–419.
81 X. Kuang, G. Liu, X. Dong and D. Wang, *Macromol. Mater. Eng.*, 2016, **301**, 535–541.
82 N. Candau, L. Chazeau, J.-M. Chenal, C. Gauthier and E. Munch, *Phys. Chem. Chem. Phys.*, 2016, **18**, 3472–3481.
83 S. Toki and B. S. Hsiao, *Macromolecules*, 2003, **36**, 5915–5917.
84 M. Bruzzone, G. Corradini and F. Amato, *Rubber Chem. Technol.*, 1966, **39**, 1593–1607.
85 P. Tanasi, M. H. Santana, J. Carretero-González, R. Verdejo and M. A. López-Manchado, *Polymer*, 2019, **175**, 15–24.
86 Y. Miwa, J. Kurachi, Y. Kohbara and S. Kutsumizu, *Commun. Chem.*, 2018, **1**, 1–8.
87 Y. Miwa, J. Kurachi, Y. Sugino, T. Udagawa and S. Kutsumizu, *Soft Matter*, 2020, **16**, 3384–3394.
88 Y. Miwa, M. Yamada, Y. Shinke and S. Kutsumizu, *Polym. Chem.*, 2020, **11**, 6549–6558.
89 X. Yang, J. Liu, D. Fan, J. Cao, X. Huang, Z. Zheng and X. Zhang, *Chem. Eng. J.*, 2020, **389**, 124448.
90 C. Xu, L. Cao, B. Lin, X. Liang and Y. Chen, *ACS Appl. Mater. Interfaces*, 2016, **8**, 17728–17737.
91 C. Xu, L. Cao, X. Huang, Y. Chen, B. Lin and L. Fu, *ACS Appl. Mater. Interfaces*, 2017, **9**, 29363–29373.
92 J. Liu, C. Xiao, J. Tang, Y. Liu and J. Hua, *Ind. Eng. Chem. Res.*, 2020, **59**, 12755–12765.
93 M. A. Rahman, L. Sartore, F. Bignotti and L. D. Landro, *ACS Appl. Mater. Interfaces*, 2013, **5**, 1494–1502.
94 Y. Liu, Z. Li, R. Liu, Z. Liang, J. Yang, R. Zhang, Z. Zhou and Y. Nie, *Ind. Eng. Chem. Res.*, 2019, **58**, 14848–14858.
95 M. A. Rahman, M. Penco, I. Peroni, G. Ramorino, A. M. Grande and L. D. Landro, *ACS Appl. Mater. Interfaces*, 2011, **3**, 4865–4874.
96 Y. Han, X. Wu, X. Zhang and C. Lu, *ACS Appl. Mater. Interfaces*, 2017, **9**, 20106–20114.
97 X. Liu, G. Su, Q. Guo, C. Lu, T. Zhou, C. Zhou and X. Zhang, *Adv. Funct. Mater.*, 2018, **28**, 1706658.
98 Y. Tang, Q. Guo, Z. Chen, X. Zhang, C. Lu, J. Cao and Z. Zheng, *ACS Appl. Mater. Interfaces*, 2019, **11**, 23527–23534.
99 Q. Guo, B. Huang, C. Lu, T. Zhou, G. Su, L. Jia and X. Zhang, *Mater. Horiz.*, 2019, **6**, 996–1004.
100 J. Liu, J. Liu, S. Wang, J. Huang, S. Wu, Z. Tang, B. Guo and L. Zhang, *J. Mater. Chem. A*, 2017, **5**, 25660–25671.
101 Y. Chen, Z. Tang, Y. Liu, S. Wu and B. Guo, *Macromolecules*, 2019, **52**, 3805–3812.
102 S. Ghorai, A. K. Jalan, M. Roy, A. Das and D. De, *Polym. Test.*, 2018, **69**, 133–145.
103 A. Birley, *Br. Polym. J.*, 1989, **21**, 362–362.
104 N. H. H. Shuhaimi, N. S. Ishak, N. Othman, H. Ismail and S. Sasidharan, *J. Elastomers Plast.*, 2014, **46**, 747–764.
105 M. Hernández, A. M. Grande, W. Dierkes, J. Bijleveld, S. Van Der Zwaag and S. J. García, *ACS Sustainable Chem. Eng.*, 2016, **4**, 5776–5784.
106 L. Imbernon, E. Oikonomou, S. Norvez and L. Leibler, *Polym. Chem.*, 2015, **6**, 4271–4278.
107 B. Cheng, X. Lu, J. Zhou, R. Qin and Y. Yang, *ACS Sustainable Chem. Eng.*, 2019, **7**, 4443–4455.
108 J. Nie, W. Mou, J. Ding and Y. Chen, *Composites, Part B*, 2019, **172**, 152–160.
109 Y. Chen, J. Nie, C. Xu, W. Wu and Z. Zheng, *ACS Sustainable Chem. Eng.*, 2019, **8**, 1285–1294.
110 J. Nie, J. Huang, J. Fan, L. Cao, C. Xu and Y. Chen, *ACS Sustainable Chem. Eng.*, 2020, **8**, 13724–13733.
111 L. Cao, D. Yuan, C. Xu and Y. Chen, *Nanoscale*, 2017, **9**, 15696–15706.
112 L. Cao, J. Fan, J. Huang and Y. Chen, *J. Mater. Chem. A*, 2019, **7**, 4922–4933.
113 M. A. Sattar, S. Gangadharan and A. Patnaik, *ACS Omega*, 2019, **4**, 10939–10949.
114 S. Utrera-Barrios, M. H. Santana, R. Verdejo and M. A. López-Manchado, *ACS Omega*, 2020, **5**, 1902–1910.
115 Q. Guo, X. Zhang, F. Zhao, Q. Song, G. Su, Y. Tan, Q. Tao, T. Zhou, Y. Yu and Z. Zhou, *ACS Nano*, 2020, **14**, 2788–2797.

116 R. N. Webb, T. D. Shaffer and A. H. Tsou, *Kirk–Othmer Encyclopedia of Chemical Technology*, 2000.
117 R. Cao, X. Zhao, X. Zhao, X. Wu, X. Li and L. Zhang, *Ind. Eng. Chem. Res.*, 2019, **58**, 16645–16653.
118 P. Xie, K. Wang, J. Zhang, Y. Hu and G. Luo, *Ind. Eng. Chem. Res.*, 2018, **57**, 10883–10892.
119 J. S. Parent, G. D. White, R. A. Whitney and W. Hopkins, *Macromolecules*, 2002, **35**, 3374–3379.
120 J. S. Parent, A. Penciu, S. A. Guillén-Castellanos, A. Liskova and R. A. Whitney, *Macromolecules*, 2004, **37**, 7477–7483.
121 G. Davidson, D. Adkinson, S. Malmberg, L. Ferrari, C. Siegers and S. Chadder, *US Pat.*, 9388258B2, 2016.
122 L. Ferrari, N. Suhan, C. Siegers and T. B. Carmichael, *US Pat.*, 9969824B2, 2018.
123 J. S. Parent, A. M. Porter, M. R. Kleczek and R. A. Whitney, *Polymer*, 2011, **52**, 5410–5418.
124 A. Ozvald, J. S. Parent and R. A. Whitney, *J. Polym. Sci., Part A: Polym. Chem.*, 2013, **51**, 2438–2444.
125 A. Das, A. Sallat, F. Böhme, E. Sarlin, J. Vuorinen, N. Vennemann, G. Heinrich and K. W. Stöckelhuber, *Polymers*, 2018, **10**, 94.
126 A. Das, A. Sallat, F. Böhme, M. Suckow, D. Basu, S. Wießner, K. W. Stöckelhuber, B. Voit and G. Heinrich, *ACS Appl. Mater. Interfaces*, 2015, **7**, 20623–20630.
127 M. Suckow, A. Mordvinkin, M. Roy, N. K. Singha, G. Heinrich, B. Voit, K. Saalwächter and F. Böhme, *Macromolecules*, 2017, **51**, 468–479.
128 A. Mordvinkin, M. Suckow, F. Böhme, R. H. Colby, C. Creton and K. Saalwächter, *Macromolecules*, 2019, **52**, 4169–4184.
129 S. Stein, A. Mordvinkin, B. Voit, H. Komber, K. Saalwächter and F. Böhme, *Polym. Chem.*, 2020, **11**, 1188–1197.
130 H. Kim, A. L. Yarin and M. W. Lee, *Composites, Part B*, 2020, **182**, 107598.
131 H. H. Le, F. Böhme, A. Sallat, S. Wießner, M. auf der Landwehr, U. Reuter, K. W. Stöckelhuber, G. Heinrich, H. J. Radusch and A. Das, *Macromol. Mater. Eng.*, 2017, **302**, 1600385.
132 H. Le, S. Hait, A. Das, S. Wiessner, K. Stöckelhuber, F. Böhme, U. Reuter, K. Naskar, G. Heinrich and H.-J. Radusch, *eXPRESS Polym. Lett.*, 2017, **11**, 230–242.
133 A. Sallat, A. Das, J. Schaber, U. Scheler, E. S. Bhagavatheswaran, K. W. Stöckelhuber, G. Heinrich, B. Voit and F. Böhme, *RSC Adv.*, 2018, **8**, 26793–26803.
134 H. Mou, F. Shen, Q. Shi, Y. Liu, C. Wu and W. Guo, *Eur. Polym. J.*, 2012, **48**, 857–865.
135 Z. Cheng, M. Yan, L. Cao, J. Huang, X. Cao, D. Yuan and Y. Chen, *Ind. Eng. Chem. Res.*, 2019, **58**, 3912–3920.
136 Z. F. Zhang, X. T. Liu, K. Yang and S. G. Zhao, *Macromol. Res.*, 2019, **27**, 803–810.
137 M. Das, S. Pal and K. Naskar, *eXPRESS Polym. Lett.*, 2020, **14**, 860–880.
138 A. C. Schüssele, F. Nübling, Y. Thomann, O. Carstensen, G. Bauer, T. Speck and R. Mülhaupt, *Macromol. Mater. Eng.*, 2012, **297**, 411–419.
139 S. Utrera-Barrios, J. Araujo-Morera, L. P. de Los Reyes, R. V. Manzanares, R. Verdejo, M. Á. López-Manchado and M. H. Santana, *Eur. Polym. J.*, 2020, 110032.
140 L. Feng, H. Zhao, X. He, Y. Zhao, L. Gou and Y. Wang, *Polym. Eng. Sci.*, 2019, **59**, 1603–1610.
141 S. Sarkar, S. L. Banerjee and N. K. Singha, *Macromol. Mater. Eng.*, 2021, DOI: 10.1002/mame.202000626.
142 H. P. Xiang, M. Z. Rong and M. Q. Zhang, *ACS Sustainable Chem. Eng.*, 2016, **4**, 2715–2724.
143 S. H. Cho, H. M. Andersson, S. R. White, N. R. Sottos and P. V. Braun, *Adv. Mater.*, 2006, **18**, 997–1000.
144 S. H. Cho, S. R. White and P. V. Braun, *Chem. Mater.*, 2012, **24**, 4209–4214.
145 H. Lu and S. Feng, *J. Polym. Sci., Part A: Polym. Chem.*, 2017, **55**, 903–911.
146 Y. Wang, L. Ding, C. Zhao, S. Wang, S. Xuan, H. Jiang and X. Gong, *Compos. Sci. Technol.*, 2018, **168**, 303–311.
147 Y. Liu, K. Zhang, J. Sun, J. Yuan, Z. Yang, C. Gao and Y. Wu, *Ind. Eng. Chem. Res.*, 2019, **58**, 21452–21458.
148 Y. Miwa, K. Taira, J. Kurachi, T. Udagawa and S. Kutsumizu, *Nat. Commun.*, 2019, **10**, 1–6.
149 A. Strąkowska, A. Kosmalska, M. Masłowski, T. Szmechtyk, K. Strzelec and M. Zaborski, *Polym. Bull.*, 2019, **76**, 3387–3402.
150 X. Zhao and J. Zhang, *React. Funct. Polym.*, 2019, **138**, 114–121.
151 H. Sun, X. Liu, S. Liu, B. Yu, N. Ning, M. Tian and L. Zhang, *Chem. Eng. J.*, 2020, **384**, 123242.
152 L. Zhao, X. Shi, Y. Yin, B. Jiang and Y. Huang, *Compos. Sci. Technol.*, 2020, **186**, 107919.
153 H. Yan, S. Dai, Y. Chen and J. Ding, *ChemistrySelect*, 2019, **4**, 10719–10725.
154 K. V. Deriabin, N. A. Ignatova, S. O. Kirichenko, A. S. Novikov and R. M. Islamova, *Polymer*, 2021, **212**, 123119.
155 J. Zhao, R. Xu, G. Luo, J. Wu and H. Xia, *J. Mater. Chem. B*, 2016, **4**, 982–989.
156 L. Zhao, B. Jiang and Y. Huang, *J. Mater. Sci.*, 2019, **54**, 5472–5483.